Accepted Manuscript

Discovery of carbazole derivatives as novel allosteric MEK inhibitors by pharmacophore modeling and virtual screening

Dandan Xi, Yan Niu, Hongyue Li, Stefan M. Noha, Veronika Temml, Daniela Schuster, Chao Wang, Fengrong Xu, Ping Xu

PII: S0223-5234(19)30553-7

DOI: https://doi.org/10.1016/j.ejmech.2019.06.027

Reference: EJMECH 11430

To appear in: *European Journal of Medicinal Chemistry*

Received Date: 25 February 2019

Revised Date: 27 May 2019

Accepted Date: 10 June 2019

Please cite this article as: D. Xi, Y. Niu, H. Li, S.M. Noha, V. Temml, D. Schuster, C. Wang, F. Xu, P. Xu, Discovery of carbazole derivatives as novel allosteric MEK inhibitors by pharmacophore modeling and virtual screening, *European Journal of Medicinal Chemistry* (2019), doi: https://doi.org/10.1016/j.ejmech.2019.06.027.

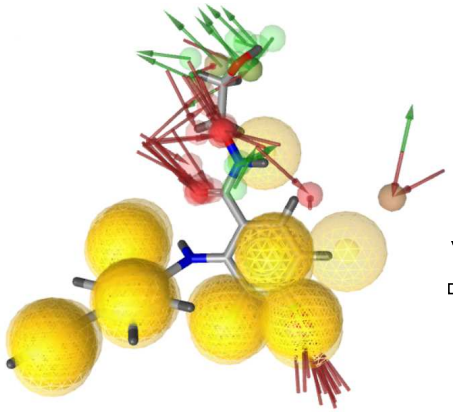

Structure-based Pharmacophore

Virtual Screening

Specs database

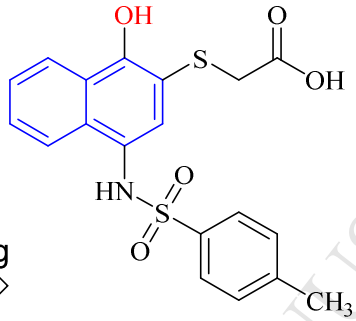

hit compound

RAF-MEK IC_{50} = 27.2 ± 4.5 μM
MTT assay IC_{50} = 8.9 ± 2.0 μM

Optimization

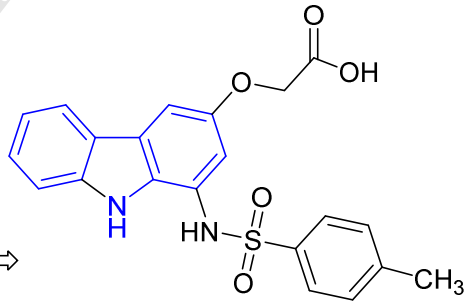

22k

RAF-MEK IC_{50} = 12.8 ± 0.5 μM
MTT assay IC_{50} > 100 μM

Discovery of Carbazole Derivatives as Novel Allosteric MEK Inhibitors by Pharmacophore Modeling and Virtual Screening

Dandan Xi[1], Yan Niu[1]*, Hongyue Li[1], Stefan M. Noha[2], Veronika Temml[2], Daniela Schuster[2,3]*, Chao Wang[1], Fengrong Xu[1], Ping Xu[1]*

[1]Department of Medicinal Chemistry, School of Pharmaceutical Sciences, Peking University Health Science Center, 38 Xueyuan Road, Beijing 100191, China.

[2]Institute of Pharmacy/Pharmaceutical Chemistry and Center for Molecular Biosciences Innsbruck, University of Innsbruck, Innrain 80-82, 6020 Innsbruck, Austria

[3]Institute of Pharmacy, Department of Pharmaceutical and Medicinal Chemistry, Paracelsus Medical University Salzburg, Strubergasse 21, 5020 Salzburg, Austria

*Corresponding authors.
Tel: +86 10 82805281. Email: yanniu@bjmu.edu.cn (Y. Niu),
Tel: +43 512 50758253. Email: daniela.schuster@uibk.ac.at (D. Schuster),
Tel: +86 10 82802632. Email: pingxu@bjmu.edu.cn (P. Xu)

Abstract

We report in this work the discovery of novel allosteric MEK inhibitors by pharmacophore modeling and virtual screening. Two out of 13 virtual hit compounds were identified as MEK kinase inhibitors using a MEK1 binding assay. Structural derivations on the hit compound **M100** (IC_{50} = 27.2 ± 4.5 μM in RAF-MEK cascading assay) by substituent transformation and bioisosterism replacement have led to the synthesis of a small library of carbazoles. The enzymatic studies revealed the preliminary structure-activity relationships and the derivative **22k** (IC_{50} = 12.8 ± 0.5 μM) showed the most potent inhibitory effect against Raf-MEK cascading. Compound **7** was discovered as toxic as **M100** to tumor cells whereas safer to HEK293 cells (IC_{50} > 100 μM) than **M100** (IC_{50} = 8.9 ± 2.0 μM). It suggests that carbazole is a good scaffold for the design of novel MEK inhibitors for therapeutic uses. More importantly, the developed pharmacophore model can serve as a reliable criterion in novel MEK inhibitor discovery.

Keywords: pharmacophore modeling; virtual screening; MEK inhibitor; carbazoles; bioisosterism

1. Introduction

Mitogen-activated protein kinases (MAPKs) are a highly conserved family of serine/threonine protein kinases involved in a variety of fundamental cellular events such as survival, proliferation, differentiation, stress response, and apoptosis[1]. In mammals, more than a dozen MAPK enzymes have been identified, among which the best known ones are the conventional MAPKs, including the extracellular signal-regulated kinases 1 and 2 (ERK1/2), c-Jun amino-terminal kinases 1 to 3 (JNK1 to 3), p38 (α, β, γ, and δ), and ERK5 families[2]. Each group of conventional MAPKs is composed of a set of three kinases, a MAPK, a MAPK kinase (MAPKK), and a MAPKK kinase (MAPKKK), which in turn phosphorylate and activate MAPKs relaying extracellular signals to intracellular responses.

The ERK1/2 signaling pathway is, by far, the best-characterized MAPK pathway consisting of the MAPKKKs A-Raf, B-Raf, and Raf-1, the MAPKKs MEK1 and MEK2, and the MAPKs ERK1 and ERK2. This pathway plays a central role in the control of cell survival and proliferation. Growth factors and mitogens use the Ras/Raf/MEK/ERK signaling cascade to transmit signals from their receptors to regulate gene expression and prevent apoptosis[3]. Components of the ERK1/2 signaling cascade are frequently mutated and highly up-regulated in cancer cells, with approximately 1/3 of human tumors expressing a constitutively activated mutant of RAS[4] and approximately 8% of tumors expressing an activated form of BRAF[5, 6]. These findings prompted the development of small molecule inhibitors targeting the ERK1/2 signaling pathway as anti-cancer agents[7]. So far, two RAF inhibitors (vemurafenib and dabrafenib) and three MEK inhibitors (trametinib, cobimetinib, binimetinib) have been approvedby the FDA of US for the treatment of melanoma expressing the mutated RAF paralogue BRAF (V600E or V600K)[8-10]. In addition, selumetinib, a highly selective MEK inhibitor has been granted Orphan Drug

Designation for adjuvant treatment of patients with stage III or IV differentiated thyroid cancer[11].

MEK1 and MEK2 are dual-specificity tyrosine/threonine proteinkinases, which play an integral role in the Ras/Raf/MEK/ERK signaling module[12].They are attractive targets for ERK1/2 pathway modulation because ERK1/2 are known to be the only substrates for MEK1/2, and MEK1/2 specific modulator could thus confine its function within the ERK1/2 pathway leaving other pathways unaffected[13]. Additionally, co-crystal structures revealed that MEK1/2 has an allosteric site[14, 15], which endows inhibitors with high selectivity against MEK1/2 by a non-ATP competitive mechanism. The binding site, which is adjacent to, but different from, the ATP-binding site undergoes several conformational changes to lock unphosphorylated MEK1/2 in a catalytically inactive state. Undesired adverse effects can be largely avoided owing to this specific binding to MEK kinase[16].

Although numerous small molecule inhibitors have been discovered within the past two decades, the diversity of the available MEK1/2 inhibitors remains limited. Most of the reported MEK1/2 inhibitors can be structurally categorized as biarylamines[17,18], for example, the FDA-approved trametinib, cobimetinib, and binimetinib, the in-clinical-trailed compounds pimasertib, refametinib, PD184352, and PD0325901 (**Fig 1**). A good degree of similarity can be seen among the majority of these inhibitors. Unlike the closely related biarylamines, the non-biarylamine inhibitors are quite dissimilar to one and another. For example, the scaffold of U0126 is a symmetric vinylogous cyanamide which undergoes cyclization and isomerization in aqueous solution[19], and mostly used as an *in vitro* laboratory tool. Derivation from PD98059 has generated a series of chromone-based inhibitors against MEK1 with IC_{50} values in nanomolar range[20]. Compound RO5126766, which is also known as CH5126766, represents a series of chromen-2-one-based dual Raf/MEK inhibitors that can suppresses feedback reactivation of RAF activity[21]. Similarly, RO5068760 and its hydantoin-based analogues can also prevent feedback reactivation in addition to MEK/ERK dual inhibition[22,23] (**Fig. 1**).

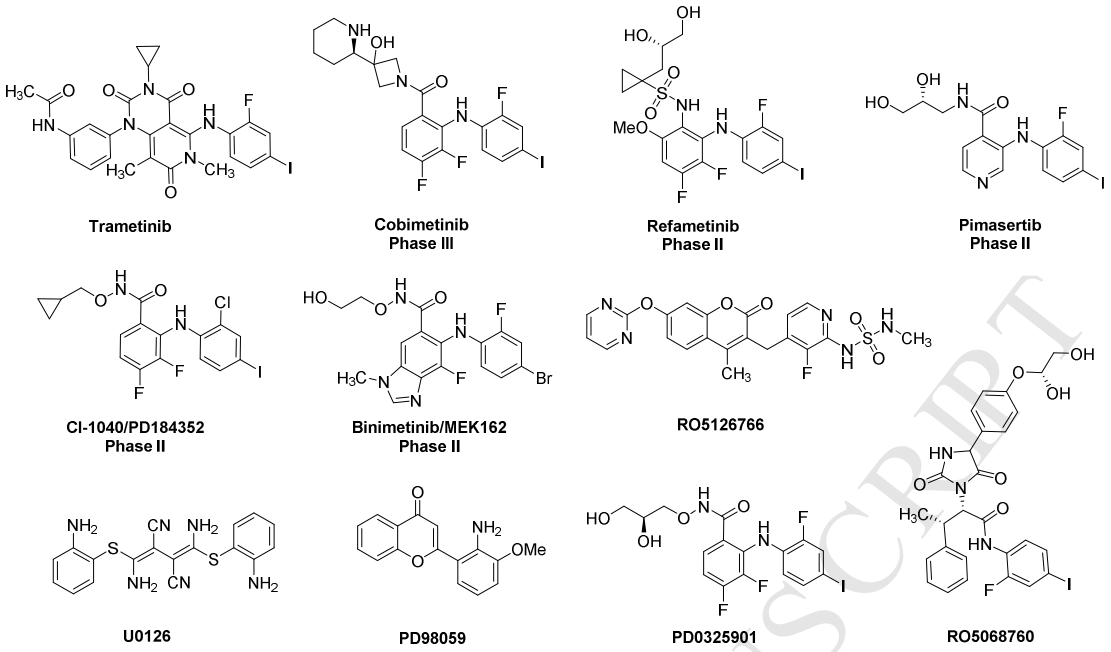

Fig. 1. Representative MEK1/2 inhibitors.

Co-crystal structure has revealed that although bind to the same allosteric site, novel non-biarylamine inhibitors like RO5126766[24], adopt binding modes different from those biarylamines. For example, the inhibitors miss some of the key interactions with Val127 or Lys97 while extending to a cavity surrounded by Arg189, Asn221, Ser222, and others. We thus wondered, if there were any novel MEK inhibitors that can not only retain the key interaction normally formed by biarylamines, but also form some additional interactions or occupy some specific sub-pockets of MEK in the allosteric site. To this end, we decided to build a pharmacophore model starting from the active conformations of biarylamines isolated from co-crystal structures in complex with MEK1, followed by analysis of the hit compounds out of database screening, and search for the MEK inhibitors with novel binding modes.

2. Results and discussion

2.1 Pharmacophore modeling and virtual screening

Up to this work was initiated, there were 45 crystal structures of MEK1 released in the Protein Data Bank[25], among which 26 were in complex with ligands closely related to biarylamines. We collected co-crystal structures of 11 classic biarylamine-MEK1 complexes to build pharmacophore models. The PDB entries of the 11

co-crystal structures[26-34] and the ligand structures are listed in **Fig 2.**

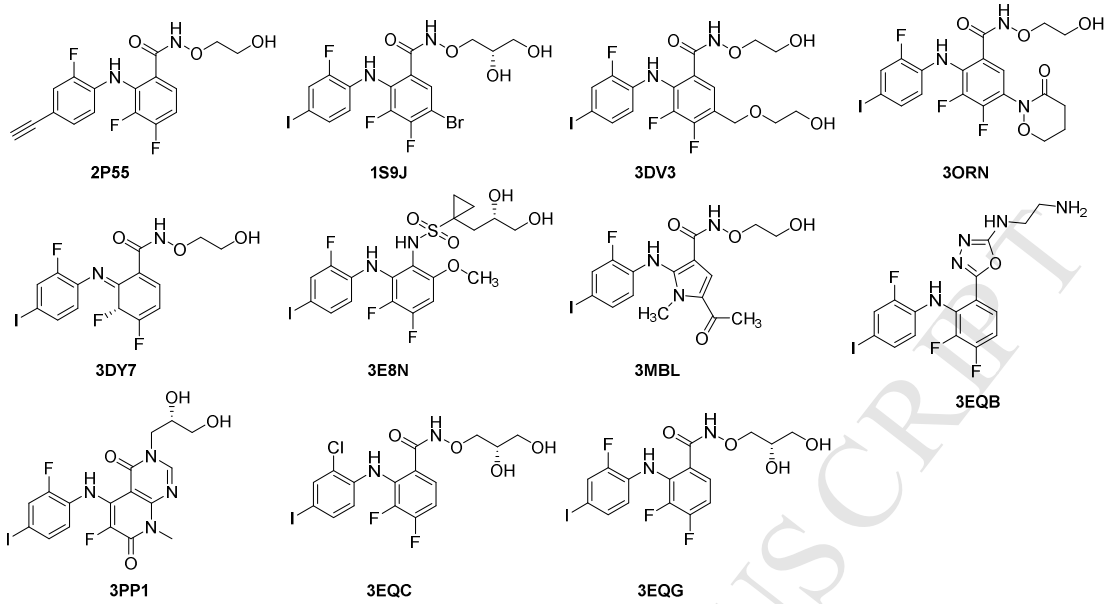

Fig. 2. The PDB entries of the 11 co-crystal and ligand structures used to build pharmacophore model.

For each of the 11 PDB complexs, a structure-based pharmacophore model was generated automatically by using the LigandScout 3.02 software[35]. All the automated models possessed 7-10 chemical features, in addition to many exclusion volumes. For example, pharmacophore model 2P55 was composed of six hydrophobic features, two hydrogen bond (HB) acceptors，and one HB donor，in addition to 19 exclusion volumes (**Fig 3a** and **3b**). Two of the six hydrophobic features were generated from the biaryl rings within the 2P55 ligand (ring A and ring B in **Fig. 3a** and **3b**). For easier description in the following context, ring A refers to the one connected with the linear side chain and ring B is the ring substituted with one or two halogens. With the aim of finding novel ligands with more structural diversity, the exclusion volumes were consequently not considered in the following model validation and database screening. The topologies of the remaining pharmacophore features of the 11 models were very similar and they overlapped very well when aligned by the “reference points” with LigandScout (**Fig 3c**).

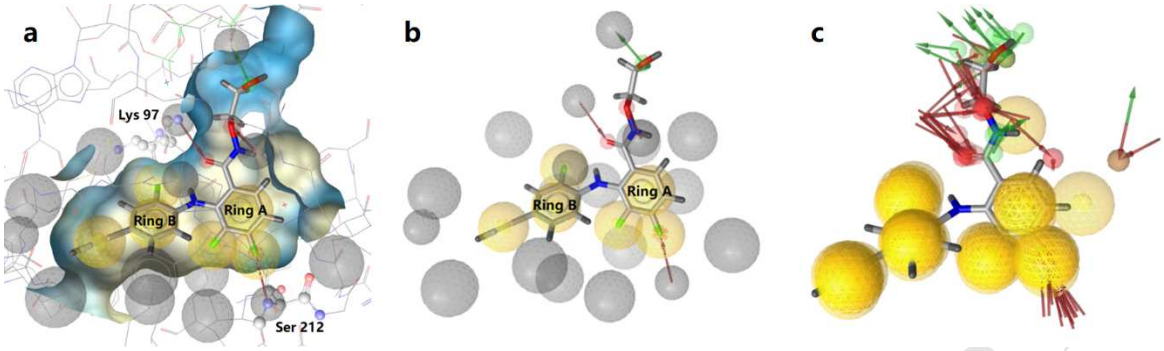

Fig. 3. Structure-based pharmacophore models generated by LigandScout. a) Alignment of 2P55 ligand with its pharmacophore model in the allosteric pocket of MEK1; b) Model from the ligand-protein complex 2P55; c) The overlapping of all eleven models. Among the features within models, yellow spheres represent hydrophobic features, red arrows represent hydrogen bond acceptors, and green arrows represent hydrogen bond donors. Exclusion volumes are shown in grey and hidden for clarity in Fig. 3c.

For model validation, we organized a test dataset composed of 142 active, 5 inactive, and 6041 decoy compounds collected from the ChEMBL Database[36]. Here, decoys refer to those compounds with reported activities not related to MEK, whereas their physical properties, including molecular weight, ALogP, number of rotatable bonds, and number of HB acceptor and donors, were similar to those of known MEK inhibitors. **Table 1** shows the values for each physical property considered in the decoy compound selection, and these values came from the analysis of the above mentioned 142 active compounds. The quality of the pharmacophore model, namely the ability to enrich the active compounds from the data set, was evaluated by calculating enrichment factors (EF) using the equation below, where *TP* is the number of active compounds fitting into the model, *n* is the total number of molecules (including both active compounds and decoys) that were returned as hits by the pharmacophore-based screening, *A* is the number of active compounds in the entire validation database, and *N* is the number of all compounds in the validation database.

$$EF = \frac{TP / n}{A / N}$$

Table 1. Physicochemical properties considered in decoy compound selection

Physical Properties	Value

Molecular Weight	≥ 400 and ≤ 500
ALogP	≥ 1.4 and ≤ 4.6
Number of Rotatable Bonds	≥ 4
Number of Hydrogen Bond Acceptors	≥ 4
Number of Hydrogen Bond Donnors	≥ 4

Possessing many features, the individual models were too specific so that almost none of the compounds in the active dataset could be correctly classified (**Table S1** in **Supporting Information**). The exceptions were models 3MBL and 3PP1, having only 7 features with no hydrophobic features on ring A (**Fig. 3b**). These two models hit more than 5 compounds in the active dataset, which indicated that the hydrophobic features on ring A might not be required for MEK inhibition. Therefore, the hydrophobic features on ring A were all deleted from each of the automated models, if present, for refinement. Based on the observation that the hydrophobic pocket formed by Met143, Ile141, Leu118 and Phe209 had relatively limited space to accommodate more of the hydrophobic substitutions on position 2 of ring B, one of the corresponding hydrophobic features was also deleted, although in most of the cases it was occupied by halogens in the biarylamine ligands. As for the HB acceptors, the number of this feature in each automated model varied from 2 to 4, among which two were shared by all models. One of them referred to the halogen or carbonyl oxygen in position 4 of ring A interacting with the peptidic backbone of Ser 212 (**Fig. 3a**), the other was the oxygen or carbonyl group on the substitution at position 2 of ring A bonding with Lys 97. These two HB acceptors seemed to be more important compared with other features, therefore, they were kept in all models during refinement.

Among the automated models, 1S9J, 3MBL and 3PP1 were observed forming one additional HB with Val 211, in adjacent to the HB formed with Ser 212. Since this HB acceptor was only observed in 3 of the 11 automated models, it was likely to be less important, thus be set as “optional” if available. In addition, Lys 97 was found forming HB with individual ligand in 1S9J, 3DV3, and 3ORN at some upper positions, and therefore, these HB acceptors were included in the refined models and were set as “optional”.

It can be seen from **Fig. 3b** that directions of the HB donor features (green arrows) varied a lot. These HBs were observed forming with ATP instead of with MEK1. These direct hydrogen bondings may restrict ATP-γS hydrolysis due to limited access to the water required for such reaction. It might not be required for MEK inhibition, because this direct hydrogen bonding with ATP was not observed in 1S9J, 3DV3, 3DY7, and 3ORN at all, and many compounds in the active dataset didn't have corresponding substructure to form this HB, either. Therefore, we set this HB donor feature as "optional" during refinement.

The refined models were used to screen the testset compounds again with results shown in **Table 2**. The enrichment factors ranged from 12.82 to 26.28, which were much more improved than those of the automated ones (**Table S1**).

Table 2 Number of hit compounds in the test set by the refined models.

Model code	No. of Hits Inactive	No. of Hits Active	No. of Hits Decoy	EF
1S9J-r-1	1	52	68	18.87
1S9J-r-2	0	8	16	14.51
2P55-r	0	67	44	26.28
3DV3-r-1	0	60	48	24.19
3DV3-r-2	0	65	42	26.45
3DY7-r	1	58	139	12.82
3E8N-r	0	74	104	18.10
3EQB-r	0	70	75	21.02
3EQC-r	0	62	84	18.49
3EQG-r	0	49	45	22.70
3MBL-r	0	57	60	21.21
3ORN-r-1	0	59	67	20.39
3ORN-r-2	0	13	14	20.97
3PP1-r	0	58	106	15.40

To indicate how the refined models could hit the active compounds, a heat map was drawn (**Fig. S1** in **Supporting Information**). Accordingly, we have tried many different combinations of the models to increase the possibility to hit more active compounds, and finally, a collection of 1S9J-r-1, 2P55-r and 3DV3-r-1 (**Fig. 4**) were selected representing all the possible binding modes of biarylamine ligands. They have hit 80 compounds in the active dataset (142 in total, 56.3% hit rate) and

generated a final EF of 17.16.

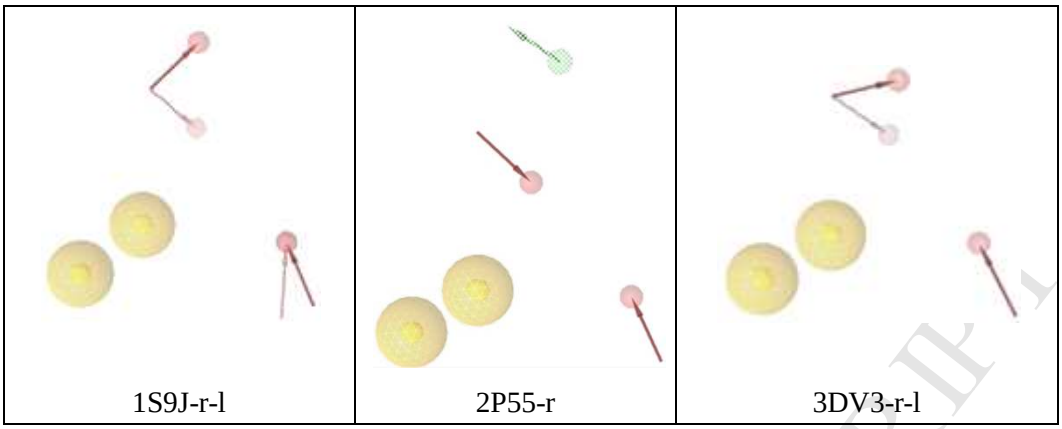

Fig. 4 The pharmacophore model collection selected for the large-scale virtual screening.

The generated collection of pharmacophore models was used for virtual screening of the Specs database (version Apr 2010, www.specs.net) containing 200,158 compounds in total. The numbers of virtual hits for each model were listed in **Table 3**.

Table 3 Number of hit compounds identified by the individual pharmacophore model in the collection.

Model name	Hits number	Hit rate %	Number of top hits selected
1S9J-r-l	507	0.25	42
2P55-r	6142	3.08	17
3DV3-r-1	3063	1.53	304

The total number of virtual hits was 507 + 6,142 + 3,063 = 9,712, among which some could be hit by more than one model. These virtual hits datasets were merged and clustered by structural similarity with Pipeline Pilot 7.5 software (Accelrys Inc., San Diego, CA, USA). Representative compounds with better lead-likeness were selected manually from the structural clusters with more members than others. Finally, 13 hit compounds (**Table 4**) were selected, and purchased from Specs for further MEK1 inhibitory evaluations.

Table 4 The 13 hit compounds selected for further validation by MEK1 inhibitory assays.

Compound name	Specs entry	Hit pharmacophore model	Pharmacophore fit score
M100	AP-906/41639971	3DV3-r-1	56.07
M101	AF-399/41703146	1S9J-r-l, 3DV3-r-1	66.42/57.49
M103	AN-988/15131219	3DV3-r-1	56.81
M104	AG-690/33045045	3DV3-r-1	57.21
M105	AP-853/42877451	3DV3-r-1	56.32
M106	AN-329/42286028	1S9J-r-l, 3DV3-r-1	66.67/55.63
M108	AG-205/03751018	1S9J-r-l, 3DV3-r-1	65.54/56.58
M109	AO-365/43113290	3DV3-r-1	55.73

M110	AO-365/43300996	3DV3-r-1	55.60
M111	AK-198/36417052	2P55-r, 3DV3-r-1	55.36/55.59
M113	AG-205/36953117	1S9J-r-l	65.77
M115	AG-690/10031030	1S9J-r-l/3DV3-r-1	66.05/46.82
M116	AK-968/13027684	1S9J-r-l, 3DV3-r-1	66.45/56.57

2.2 Validation of the computational work by *in vitro* enzymatic assays

After all compounds were collected, their ability to bind with phosphorylated MEK1 was firstly measured by LanthaScreen® Eu Kinase Binding Assay. Then, to further validate their potency to inhibit the Raf-MEK-ERK signaling, both Raf-MEK and MEK-ERK cascading assay were performed at the enzymatic level.

Table 5. Results of *in vitro* enzymatic assays[a]

	Binding assay normalized to AZD6244 at 100 μM (%inhibition)		Raf-MEK cascading inhibition		MEK-ERK cascading inhibition	
Compound	20 μM (%)	2 μM (%)	20 μM (%)	2 μM (%)	20 μM (%)	2 μM (%)
U0126	-	-	87.4 ± 4.4	41.7 ± 4.9	80.9 ± 1.2	26.9 ± 1.0
M100	90.3 ± 3.9	32.1 ± 0.6	56.1 ± 6.6	4.4 ± 2.6	32.0 ± 8.5	3.9 ± 2.3
M101	35.6 ± 2.9	32.6 ± 0.7	22.6 ± 7.6	5.1 ± 8.6	29.8 ± 9.1	-10.4 ± 2.0
M103	14.4 ± 0.1	8.7 ± 0.5	49.4 ± 4.6	10.5 ± 2.9	10.4 ± 1.8	-0.9 ± 2.2
M104	29.6 ± 2.4	9.6 ± 0.3	40.7 ± 6.9	5.2 ± 2.3	13.7 ± 4.2	-5.4 ± 3.1
M105	16.2 ± 0.5	8.0 ± 0.1	32.1 ± 5.9	-7.1 ± 3.6	26.7 ± 5.8	3.3 ± 1.9
M106	39.3 ± 1.8	23.4 ± 0.0	45.7 ± 5.3	11.7 ± 5.5	12.7 ± 3.5	-1.6 ± 2.2
M108	-128.1 ± 0.5	-50.2 ± 0.4	31.9 ± 6.0	7.8 ± 1.9	6.0 ± 2.9	-3.7 ± 2.1
M109	13.52 ± 0.3	14.8 ± 0.3	32.8 ± 1.3	4.1 ± 0.5	15.2 ± 3.3	-12.1 ± 1.8
M110	34.5 ± 1.5	8.9 ± 0.7	35.0 ± 2.7	7.2 ± 3.7	8.6 ± 5.3	4.1 ± 8.2
M111	22.9 ± 1.7	4.7 ± 1.3	32.3 ± 3.5	-0.04 ± 4.3	19.9 ± 8.2	-13.1 ± 1.9
M113	28.0 ± 2.3	12.9 ± 0.3	35.1 ± 8.9	0.2 ± 9.6	3.2 ± 9.7	-17.5 ± 7.8
M115	60.1 ± 4.1	11.9 ± 1.3	57.0 ± 6.5	6.3 ± 4.4	35.0 ± 7.5	5.1 ± 1.4
M116	24.4 ± 0.6	26.1 ± 0.2	58.2 ± 4.8	14.7 ± 4.2	11.7 ± 6.1	-2.9 ± 2.3

[a] All values are an average of three parallel experiments. [b]ND stands for not determined.

Among all the 13 tested compounds, M100 and M115 showed the desired

activities (for the alignment of the two compounds with the refined pharmacophore model refer to the **Supporting Information Fig. S2**). M100 showed 90% affinity to pMEK compared to the biarylaminal inhibitor AZD6244 (selumetinib), and both M110 and M115 inhibited Raf-MEK cascading by more than 50%. Therefore, we measured the IC_{50}s for the two compounds in each of the assays. The chemical structures of M100 and M115 and the respective IC_{50}s are depicted in **Figure 5**.

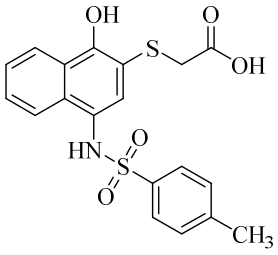

M100

RAF-MEK $IC_{50} = 27.2 \pm 4.5$ μM

MEK-ERK $IC_{50} > 160.0$ μM

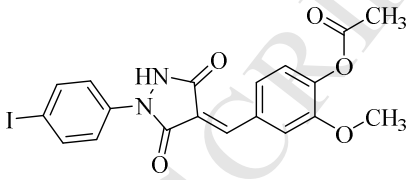

M115

RAF-MEK $IC_{50} = 25.6 \pm 1.8$ μM

MEK-ERK $IC_{50} = 63.1 \pm 5.0$ μM

Fig. 5 The chemical structures of active hit compounds and their IC_{50}s for RAF-MEK and MEK-ERK cascade inhibition.

In the following part of this paper, we report the preliminary deviations on **M100** in order to further validate the reliability of **M100** as a MEK inhibitor.

2.3 Design and synthesis of carbazoles derived from active hit compound M100

As a commercially available compound, there are already some existing reports about the bioactivities of **M100** which is a moderate proteasome inhibitor against β5 subunit[37] and its derivatives bearing a naphthol scaffold are selective Mcl-1 inhibitors[38]. Before we started our chemical deviations on **M100** toward improved potency against MEK1, its cytotoxicity was measured in CellTiter-Glo® luminescent cell viability assay[39] by using the HEK293 cell line. Results showed that **M100** was cytotoxic ($IC_{50} = 8.89 \pm 2.0$ μM), which is highly possibly related to the naphthol core within its structure.

Therefore, we started our work from replacing the naphthol scaffold with carbazole with considerations including: 1) carbazole could be regarded as a "ring-closure" form of biarylamine which is a classic structure in allosteric MEK1 inhibitors; 2) the carbazole scaffold was found in many synthetic therapeutic agents,

e.g. a blocker of β-adrenergic receptor, and regarded as a privileged structure for drug discovery[40]. Focused design and modifications on the side chain at the 3-position of the carbazole core and the sulfonamide moiety were made with the aim to explore the structure-activity relationship against MEK1.Through substituent transformation and bioisosterism replacement, the sulfur atom on the side chain was designed and replaced by an oxygen or a sulfonyl group (SO_2), while substitutes for carboxyl group included ester (COOEt), amide ($CONH_2$), or a variety of heterocycles[41]. The structures of the designed carbazole derivatives were summarized in **Figure 6**.

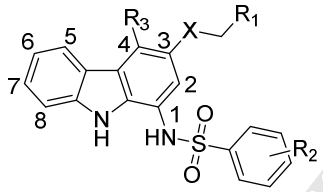

X = O, S, SO_2; R_1 = COOH, tetrazole, 3-methyl-1,2,4-oxadiazole, 5-methyl-1,3,4-oxadiazole, 5-amino-1,3,4-oxadiazole, COOEt, $CONH_2$; R_2 = *p*-Me, *p*-NHAc, *m*-NHAc; R_3 = H, OH.

Figure 6. Structure and substituted groups of designed carbazole derivatives.

M100 was synthesized following a reported procedure[42] in 2 steps (**Scheme 1**). Commercially available *p*-toluenesulfonamide was regio-selectively coupled to naphthoquinone intermediate **1** in the presence of titanium (IV) chloride and triethylamine with microwave assisted heating. Substitution of the sulfonamide intermediate **2** with thioglycolic acid as a nucleophile was carried out in presence of pyridine. After reduction *in situ* with $Na_2S_2O_4$, **M100** was obtained in a yield of 74.1%.

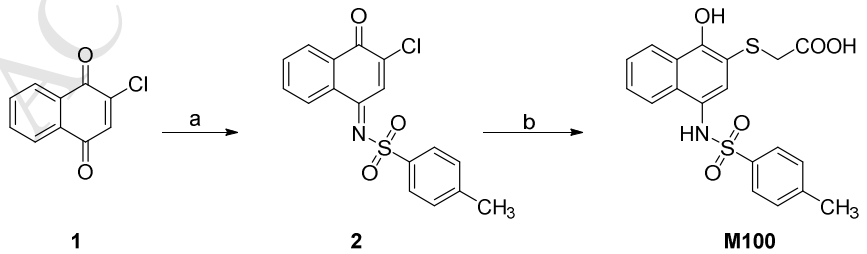

Reagents and conditions: (a) $TsNH_2$, 1 M $TiCl_4$ in DCM, Et_3N, THF, microwave, 65 °C, 15 min, 58.6%; (b) i) thioglycolic acid,pyridine, THF, r.t., 30 min; ii) $Na_2S_2O_4$, EtOAc, and H_2O (mixing in a separating funnel), r.t., 74.1%.

Scheme 1. Synthetic route of **M100**

As shown in **Scheme 2**, 4-hydroxycarbazole derivative **7** was prepared in 4 steps. Starting from **3** and N-chlorosuccimide (NCS)[43], 4-hydroxycarbazole chloride **4** was yielded, which was further oxidized to afford carbazole-1,4-dione **5**[44]. Following the same two-step procedure for **M100** synthesis, intermediate **5** was converted to desired derivative **7**.

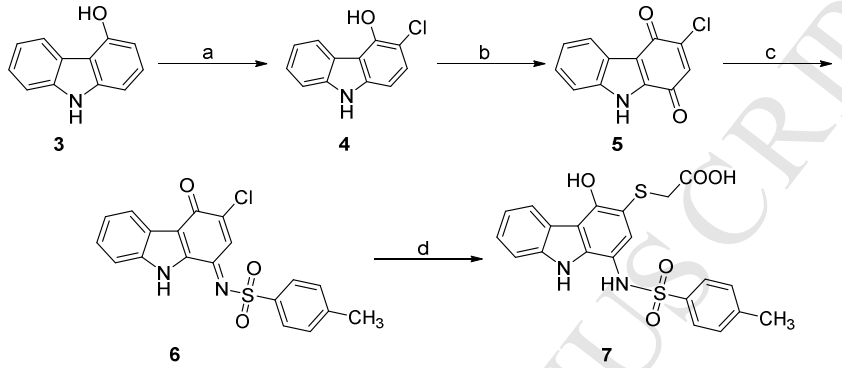

[a]**Reagents and conditions**: (a)N-chlorosuccimide (NCS), MeCN, r.t., 1.5 h, 47.6%; (b) Fremy's Salt, KH_2PO_4, water-acetone, r.t., 1.5h, 94.7%; (c) $TsNH_2$, 1 M $TiCl_4$ in DCM, Et_3N, THF, microwave, 65 °C, 15 min, 69%; (d) i) thioglycolic acid,pyridine, THF, r.t., 30 min; ii) $Na_2S_2O_4$, EtOAc, and H_2O (mixing in a separating funnel), r.t., 21.3%.

Scheme 2. Synthetic route of derivative with a 4-hydroxycarbazole core[a]

The key steps for preparation of key intermediates **12**, **14** and **15** were shown in **Scheme 3**. Reaction of 4-amino-3-nitro-phenol **8** with ethyl 2-bromoacetate in the presence of base (K_2CO_3) provided amine **9**[45] which was then diazotized and reduced to yield a substituted hydrazine analogue **10**[46]. Fischer indolization between hydrazine **10** and cyclohexanone occurred subsequently to afford tetrahydrocarbazole **11**[47]. Then, oxidation of **11** by 2,3-dichloro-5,6-dicyano-1,4-benzoquinone (DDQ) was conducted to give key intermediate **12**[48]. After hydrolysis of the ester **12** with LiOH[49], the resulting carboxylic acid **13** was then treated with acetamide oxime, EDCI and HOBt to afford key intermediate **14**[50]. Ring-closure reaction between **13**, acetohydrazide and $POCl_3$ gave key intermediate **15**[51].

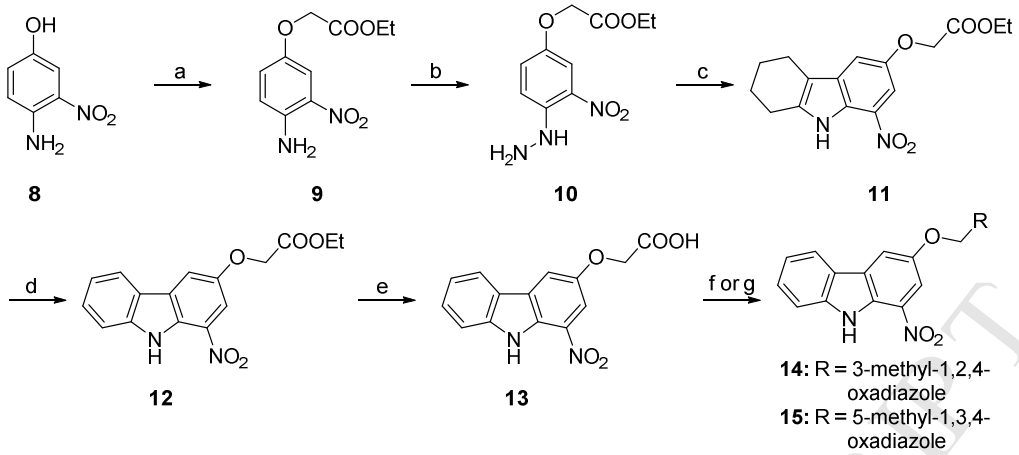

8 9 10 11 12 13

Reagents and conditions: (a) $BrCH_2COOEt$, K_2CO_3, acetone, r.t., overnight, 75.2%; (b) i) $NaNO_2$, conc. HCl, -10 °C, 0.5 h; ii) $SnCl_2$, r.t., overnight; (c) cyclohexanone, EtOH/conc. HCl (1:1), reflux, 3h, 41.7%; (d) DDQ 2.4 equiv., PhMe, reflux, 2 h, 96.2%; (e) LiOH, THF/water, r.t., 4.5 h, 99.8%; (f) HOBt, EDCI, acetamide oxime, MeCN, r.t., 0.5h, then reflux overnight, Ar, 53.8%; (g) i) acetohydrazide, HOBt, EDCI, DMF, r.t., 12h, 74.7%; ii) $POCl_3$, sealed tube, 100 °C, 1h, 65.8%.

Scheme 3. Synthetic Route to key intermediates **12**, **14**, **15**

Key intermediate **21** was synthesized through another route in 5 steps (**Scheme 4**). Compound **16** underwent diazotization, reduction and Fischer indolization to give tetrahydrocarbazole **18**, which was converted into carbazole **20** after esterification[52] and aromatization with DDQ. Finally, key intermediate **21** was generated through coupling reaction using palladium catalyst[53].

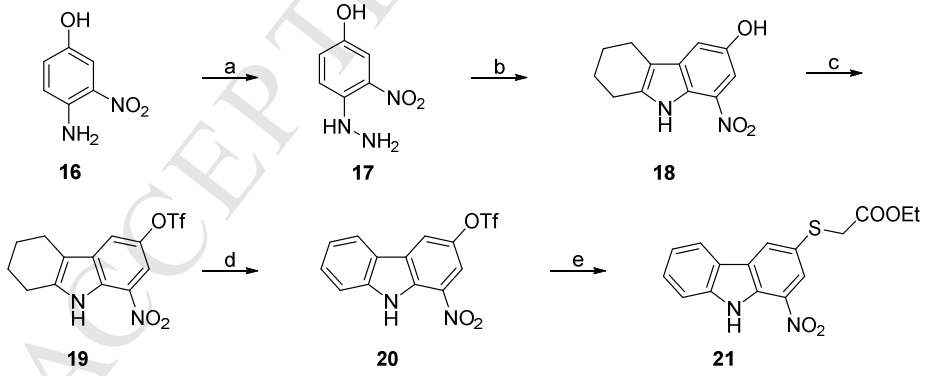

16 17 18 19 20 21

Reagents and conditions: (a) i) $NaNO_2$, conc. HCl, -10 °C, 0.5 h; ii) $SnCl_2$, r.t., 3h; (b) cyclohexanone, EtOH, reflux, overnight, 38.1%; (c) Tf_2O, 2,6-Lutidine, DCM, Ar, r.t., 24 h, 99.3%; (d) DDQ, PhMe, reflux, overnight, 77.5%; (e) $Pd_2(dba)_3$ 0.25 equiv. , Xantphos 0.5 equiv. , DIPEA, ethyl mercaptoacetate, 1,4-dioxane, Ar, reflux, overnight, 75.6%.

Scheme 4. Synthetic Route to Key Intermediates 21

With key intermediates (**12**, **14**, **15**, **21**) in hand, synthesis of a series of final compounds (**22a**, **22b**, **22c**, **22d**, **22e**, **22f**, **22g** and **22h**) were accomplished (**Scheme**

5) by reduction of -NO_2 to -NH_2 and substitution with diverse sulfonyl chlorides[54]. Corresponding carboxylic acid **22i**, **22j** and **22k** were generated from the hydrolysis of ester **22g**, **22h** and **22a**[49]. Aminolysis of **22a** with NH_4OH provided carboxamide **22l**. And then, terminalamide **221** was easily converted to tetrazole **22m** following a reported procedure[38]. 5-amino-1,3,4-oxidiazole **22o** was generated from **22a** by using a 2-step method[55]. By oxidation with oxone[42], thioether **22g** was converted to sulfone **22p** which underwent hydrolysis to provide carboxylic acid **22q**. All structures were confirmed by ^1H and ^{13}C-NMR spectroscopy, EI-MS or EI-HRMS spectra (for details, see **Experimental Section**).

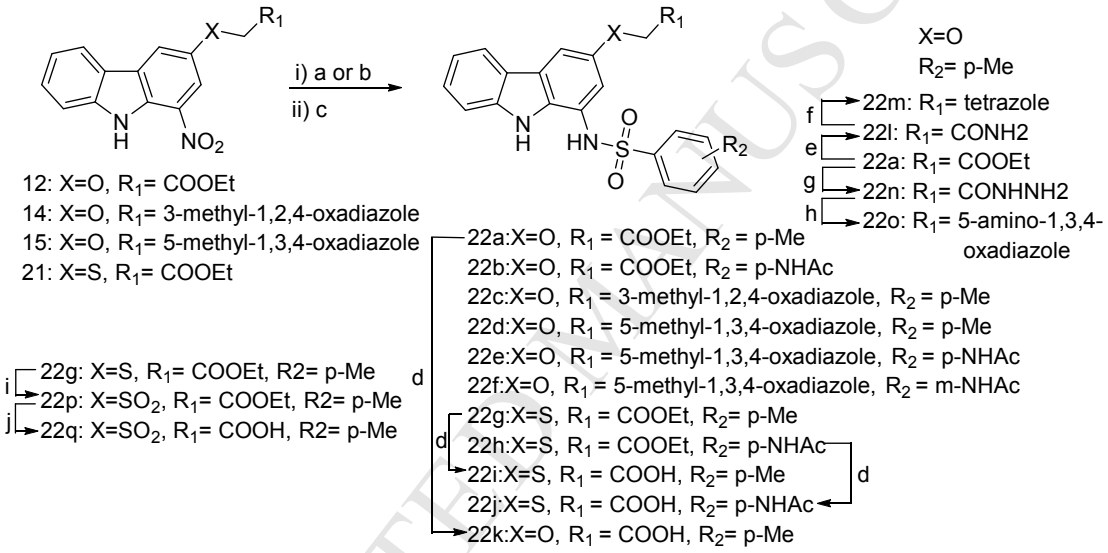

Reagents and conditions: (a) Pd-C, H_2, MeOH, r.t., overnight; (b) $Na_2S_2O_4$, K_2CO_3, DCM/MeOH, water, r.t., 2 h, Ar; (c) R_2PhSO_2Cl, pyridine, r.t., overnight, 21.6-63.9%; (d) NaOH (1N), THF/water, r.t., 1h, 88.4%; (e) NH_4OH (25%), r.t., 1 h, 94.9%; (f) NaN_3, $SiCl_4$, CH_3CN(dry), sealed tube, 80 °C, 14 h, Ar, 62.1%; (g) hydrazine hydrate, EtOH, reflux, 1 d, 83.0%; (h) BrCN, EtOH, reflux, 3 h, 22.8%; (i) oxone, acetone/water, r.t., overnight, 49.3%; (j) NaOH (1N), THF/water, r.t., 1h, 87.7%.

Scheme 5. Synthetic Route to Final Compounds

2.4 Biological evaluations and preliminary SAR of carbazole derivatives as MEK1 inhibitors

After all designed compounds were prepared, they were analyzed with the Raf-MEK and MEK-ERK cascading assays and the results were listed in **Table 6.** For Raf-MEK cascading, they were first tested at 20 μM and the IC_{50} values were determined for the 5 compounds with inhibition >50% and the best IC_{50} value (12.8 μM) was observed from **22k** and **22i**. None of the acquired compounds exhibited >50%

inhibition against MEK-ERK cascading, which was in agreement with their postulated mechanism that the allosteric MEK kinase inhibitors were supposed to inhibit MEK phosphorylation in Raf-MEK assay, instead of inhibiting the process of phosphorylated MEK to activate ERK in MEK-ERK assay.

Table 6. Inhibition of Raf-MEK and MEK-ERK cascading.

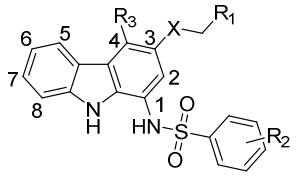

Compd.	X	R_1	R_2	R_3	Raf-MEK		MEK-ERK
					% Inhibition (20 μM)	IC_{50} ± SD (μM)	% Inhibition (20 μM)
U0126					86.2 ± 2	0.21± 0.02	85.8 ± 5.7
M100	-	-	-	-	53.1 ± 2.5	27.2 ± 4.5	12.7 ± 3.2
7	S	COOH	*p*-Me	OH	43.7 ± 0.2	31.7 ± 1.3	35.6 ± 14.6
22a	O	COOEt	*p*-Me	H	56.6 ± 0.7	23.7 ± 0.7	28.9 ± 4.9
22b	O	COOEt	*p*-NHAc	H	27.4 ± 2.7	ND[a]	18.2 ± 2.1
22k	O	COOH	*p*-Me	H	65.8 ± 3.9	12.8 ± 0.5	21.5 ± 2.7
22l	O	$CONH_2$	*p*-Me	H	41.9 ± 3.3	ND	27.9 ± 1.9
22m	O		*p*-Me	H	46.8 ± 0.3	ND	45.1 ± 13.4
22o	O	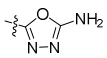	*p*-Me	H	33.0 ± 3.8	ND	21.4 ± 8.6
22c	O	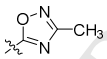	*p*-Me	H	38.2 ± 2.2	ND	37.8 ± 15.9
22d	O	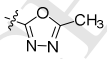	*p*-Me	H	48.6 ± 3.1	ND	25.8 ± 9.6
22e	O	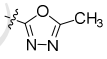	*p*-NHAc	H	50.7 ± 1.2	15.3 ± 0.6	20.6 ± 8.3
22f	O	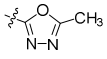	*m*-NHAc	H	29.5 ± 0.1	ND	-10.0 ± 9.6
22g	S	COOEt	*p*-Me	H	45.2 ± 2.5	ND	39.2 ± 0.2
22h	S	COOEt	*p*-NHAc	H	35.8 ± 4.0	ND	21.8 ± 0.7
22i	S	COOH	*p*-Me	H	67.2 ± 0.0	12.8 ± 1.9	21.4 ± 2.1
22j	S	COOH	*p*-NHAc	H	44.2 ± 0.0	ND	27.7 ± 7.5
22q	SO_2	COOH	*p*-Me	H	45.0 ± 4.4	ND	35.5 ± 11.6

[a] ND = not determined.

Compared with the starting compound **M100** (IC_{50} = 27.2 μM), hopping of the naphthol core with carbazole maintained the inhibitory activity (Compd. **7**, IC_{50} = 31.7 μM). As for the various $\mathbf{R_1}$, compounds with a carboxyl group (**22k**) demonstrated the best activity (IC_{50} = 12.8 μM), and the sequence of the substituents for inhibitory activity was COOH (**22k**) > COOEt (**22a**)> $CONH_2$ (**22l**) and heterocycles. As for the various $\mathbf{R_2}$, phenyl ring with an acetylamino group substituted at *para*-position (**22e**) showed better potency than *meta*- position (**22f**). Compounds with a methyl group at *para*-position of the phenyl ring (**22a**, **22g**) were more favorable than the acetylamino substituted ones (**22b**, **22h**), suggesting that steric hindrance on $\mathbf{R_2}$ might reduce binding affinity. Substitution of -OH at R_3 seemed not contribute much to the activity because compared with comd. **7** (IC_{50} = 31.7μM), **22i** demonstrated even slightly improved potency (IC_{50} = 12.8 μM). Compounds with either a thioether side chain or an ether side chain at position 3 displayed equal inhibitory activity (**22k** and **22i**, IC_{50} = 12.8 μM). However, replacement of the S or O atom by sulfonyl group (**22q**) has led to a total lost of activity. This is supposed due to the lost of flexibility of this side chain.

The above five active carbazoles were further measured for cytotoxicity against HEK293 cells, and their anti-proliferation effects were also evaluated against representative cancer cells lines, A549, A375 and HL60, with data listed in **Table 7**. As expected, all five carbazoles exhibited much reduced cytotoxicity compared with **M100**. Interestingly, although the phenolic -OH was retained as $-R_3$ in compd. **7**, its cytotoxicity remained very low with IC_{50} higher than 100 μM. In addition, the anti-proliferation effects of compd. **7** in tested cell lines were also comparable to those of **M100**. The above results have confirmed our speculation that carbazole is a better scaffold than naphthol to develop druggable molecules.

Table 7. The anti-proliferative and cytotoxic profiles [a] and docking scores of selected compounds.

	IC_{50} [b] (μM)

Compd.	HEK293	A549	A375	HL60	Glide gscore
DMSO	>100	>100	>100	>100	-
Staurosporine	0.0037 ± 0.0010	-	-	-	-
U0126	-	32.2 ± 7.5	1.1 ± 0.2	0.3 ± 5.3	-
M100	8.9 ± 2.0	21.6 ± 6.1	7.7 ± 1.1	17.2 ± 6.6	-5.302
7	>100	12.8 ± 1.9	14.7 ± 0.6	26.3 ± 3.4	-7.677
22a	>100	70.7 ± 0.9	70.7 ± 0.9	>100	-7.369
22k	>100	>100	>100	>100	-7.95
22e	>100	>100	43.7 ± 0.6	>100	-6.28
22i	>100	>100	>100	>100	-6.28

[a]The cytotoxicity was measured on HEK293 cells; [b]IC_{50} values are the means of three independent experiments.

2.5 Effect of ATP concentrations on the Raf-MEK cascading inhibitory potency

The ATP competitive profile of these inhibitors was evaluated by using representative compound **22k** in BRaf/MEK1 cascade inhibition assay by varying ATP concentrations. The IC_{50} values were 13.2 μM and 12.1 μM respectively when the ATP concentration varied from 100 μM to 300 μM. No shift in IC_{50} (**Figure 7**) was observed when ATP concentration was even increased up to 300 μM, and it suggested that compound **22k** inhibited the BRaf/MEK1 cascading in an ATP non-competitive manner.

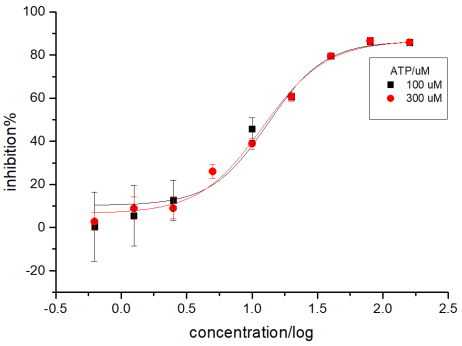

Figure 7. The dose-response curve of **22k** in BRaf-MEK cascading assay at various ATP concentrations

2.6 Docking Studies

Both the virtual hit **M100** and several selected derived carbazoles were docked into the allosteric site MEK1 (PDB entry: 3DV3) by using Schödinger suite 2016-2 (Schrödinger, LLC, New York, NY, USA) to evaluate the binding modes. As shown in

Table 7, a significantly improved docking score was achieved by **22k** (-7.950) compared with **M100** (-5.302). Three HBs were observed forming between **M100** and MEK1, among which two were formed by the sulfonyl oxygen with Lys97, and the other was between the carboxylic oxygen and Asp 208 (**Fig. 8a**). However, the orientation of the 4-methylbenzenesulfonamide moity within **22k** was reversed, and therefore, the HB with Lys97 was formed by the carboxylic oxygen of **22k**. The increased binding affinity of **22k** was supposed largely due to the additional HBs formed by the carbazole and sulfomide nitrogen with Phe209, together with two additional π - π stacking between the carbazole ring and Phe209 (**Fig. 8b**). The sulfonyl oxygen of **22k** was also observed forming critical HB with Ser212. In summary, it seemed that the binding of **22k** was more favorable than the lead compound **M100**. To further increase affinity based on **22k**, halogen can be introduced to the carbazole ring to mimic the halogen bond formed by the native ligand of 3DV3 and Val127. Alternatively, negative charged substitutions can be introduced at the *para*-position of the benzenesulfonamide moity of **22k** to fit into the positive charge pocket unoccupied.

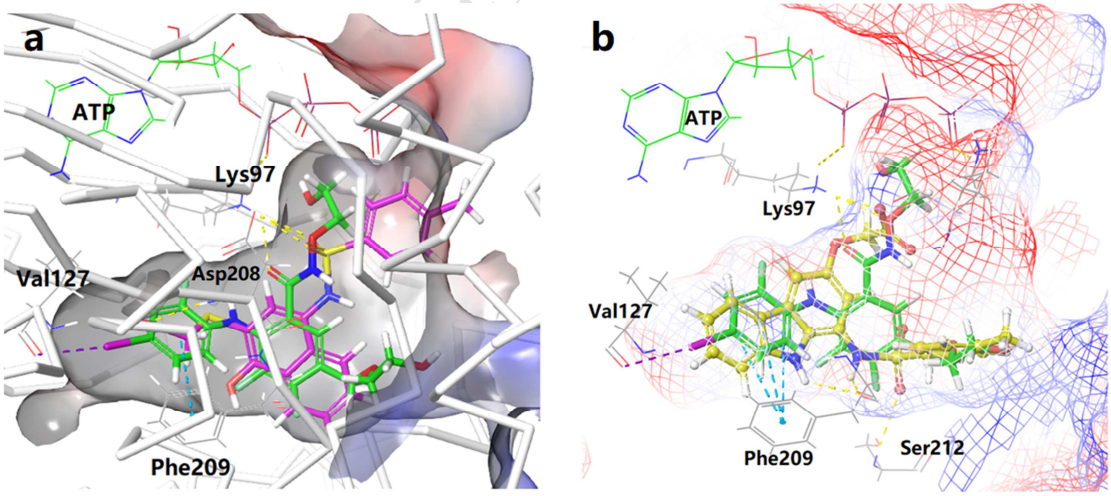

Fig. 8 The predicted binding mode of **M100** (**a**) and **22k** (**b**) with MEK1 (PDB entry: 3DV3) in the allosteric site. The native ligand of 3DV3 is presented in green sticks, while **M100** in purple and **22k** in yellow. The hydrogen bonds are shown in yellow dashed lines, and the magenta dashed lines represent halogen bond. The surface of the binding site is shown either in solid or mesh in which red represent negative charge and blue represent positive charge.

3. Conclusions

A structure-based pharmacophore model of MEK1 inhibitors was constructed and used as the criterion in a large scaled virtual screening. Two active compounds with moderate potency were identified as novel MEK inhibitors out of 13 virtual hits. Deviations on one hit, **M100**, by using substituent transformation and bioisosterism replacement, have generated several active carbazole derivatives with IC_{50}s at μM level against Raf-MEK cascading, and with greatly reduced cytotoxicity to HEK293 cells. These results suggested the liability of our pharmacophore models, and that carbazole can serve as a good starting point of novel MEK1 inhibitor design.

4. Experimental section

4.1 Computational works

The pharmacophore models were generated with LigandScout 3.02 software which is a useful tool for generating 3D pharmacophore models from structural data of macromolecular complexes, and the models generated can either be manually refined or directly used to screen databases.

The physicalchemical properties of compounds were calculated by using "Calculate Molecular properties" function within Discovery Studio software (Accelrys, Discovery Studio Vers. 2.5, San Diego, CA, USA.). Clustering was performed with the "Find Diverse Molecules" function by using the predefined set FCFP4 for fingerprint comparison. For filtering and analysis of libraries, Accelrys' Pipeline Pilot (PP) version 7.5 was used.

Docking studies were performed in Schödinger Suite (Schrödinger, LLC, New York, NY, USA) using the standard precision mode and the co-crystallized ligand of PDB entry 3DV3 [28] as center of the grid box.

4.2 Chemistry

Melting points were measured with an X4 apparatus and were uncorrected. ^{1}H NMR spectra were recorded on a Bruker (BrukerBioSpin AG, Fällanden, Switzerland) Avance III 400 MHz system. Chemical shifts were reported in parts permillion (ppm) relative to tetramethylsilane (TMS) as internal standard. The spin multiplicities were

given as s (singlet), d (doublet), t (triplet), q (quartet), m (multiplet) or br (broad). MS and high-resolution mass spectra (HRMS) were obtained using Electrospray Ionization (ESI) technique on a Bruker's Fourier Transform Ion Cyclotron resonance Mass Spectrometer. Thin layer chromatography (TLC) analysis was performed on silica gel GF254 purchased from Qingdao Haiyang Chemical Co. (Qingdao, Shandong Province, China) or Merck (Darmstadt, Germany).

4.2.1 *N-(3-chloro-4-oxonaphthalen-1(4H)-ylidene)-4-methylbenzenesulfonamide* (**2**)

To a suspension of $TsNH_2$ (1.37 g, 8 mmol) and 2-chloro-1,4-naphthoquinone (1.54 g, 8 mmol) in dry THF (65 mL) in an ice bath, 1 M $TiCl_4$ solution in DCM (8 mL) was added dropwise, followed by addition of TEA (2.64 mL, 17.6 mmol). The mixture was heated to 65 °C under microwave irradiation for 15 min. Then, inorganic salts were filtered off. The filtrate was concentrated and purified by column chromatography (silica gel, DCM/PE = 1/2) to afford a yellow solid (1.62 g, 58.6%). m.p.: 135-136 °C. ^{1}H NMR (400 MHz, DMSO-d_6): δ 8.44 (s, 1H, ArH), 8.07-8.11 (m, 2H, ArH), 7.97 (d, J = 8.28Hz, 2H, ArH), 7.81-7.89 (m, 2H, ArH), 7.53 (d, J = 8.04Hz, 2H, ArH), 2.45 (s, 3H, CH_3).

4.2.2 *2-((1-hydroxy-4-(4-methylphenylsulfonamido)naphthalen-2-yl)thio)acetic acid* (**M100**)

Intermediate **2** (345.5 mg, 1 mmol), thioglycolic acid (0.11 mL, 1.5 mmol) and pyridine (0.12 mL, 1.5 mmol) were mixed in THF (12 mL) and stirred at room temperature for 0.5 h. After the solvent was removed *in vacuum*, the residue was dissolved in EtOAc (50 mL) and was transferred to a separation funnel. The organic phase was washed with $KHSO_4$ solution (0.5 M, 50 mL) twice to remove excess pyridine, and the aqueous phase was removed. $Na_2S_2O_4$ (1.04 g, 5 mmol) and water (50 mL) was added, and the organic phase was shaken to colorless before was collected and washed with water (50 mL), brine in sequence and dried over anhydrous Na_2SO_4. The organic phase was concentrated and the residue was recrystallized to obtain a white solid (298.9 mg, 74.1%). m.p.: 153-154 °C. ^{1}H NMR (400 MHz,

DMSO-d_6): δ 12.82 (s, 1H, COOH), 9.84 (s, 1H, $SO_2N\underline{H}$), 8.13 (d, J = 8.00 Hz, 1H, ArH), 7.93 (d, J = 7.60 Hz, 1H, ArH), 7.52 (d, J = 8.40 Hz, 2H, ArH), 7.50-7.42 (m, 2H, ArH), 7.30 (d, J = 8.00 Hz, 2H, ArH), 6.95 (s, 1H, ArH), 3.47 (s, 2H, CH_2), 2.34 (s, 3H, CH_3). ^{13}C NMR (100 MHz, DMSO-d_6): δ 171.53, 152.47, 143.43, 137.31, 131.62, 129.93, 129.32, 127.42, 127.11, 126.26, 125.51, 124.79, 123.96, 122.79, 113.40, 37.19, 21.43. ESI-MS ($C_{19}H_{17}NO_5S_2$): m/z 402.12 (M-H^+); HRMS (ESI$^-$) m/z calculated for $C_{19}H_{16}NO_5S_2$ (M-H)$^-$: 402.04699, found 402.04754.

4.2.3 *3-chloro-9H-carbazol-4-ol* (**4**)

To a solution of 9*H*-carbazol-4-ol (918.2mg, 5mmol) in acetonitrile (20 mL), NCS (667.4mg, 5mmol) was added portionwise in more than 10 min. The reaction mixture was stirred at ambient temperature for 1.5 h before being concentrated under reduced pressure. The residue was then purified by column chromatography over silica gel (gradient eluent = DCM/PE: 1/5-1/2). 3-chloro-carbazol-4-ol was collected as a white solid (518.2mg, 47.6%). m.p.: 218-219 °C. ^{1}H NMR (400 MHz, DMSO-d_6): δ 11.31 (s, 1H, NH), 9.78 (s, 1H, OH), 8.21 (d, J = 8 Hz, 1H, ArH), 7.46 (d, J = 8 Hz, 1H, ArH), 7.36 (td, J = 1.16 Hz J = 8 Hz, 1H, ArH), 7.30 (d, J = 8 Hz, 1H, ArH), 7.16 (td, J = 0.96 Hz J = 8 Hz, 1H, ArH), 7.00 (d, J = 8 Hz, 1H, ArH). ^{13}C NMR (100 MHz, DMSO-d_6): δ 148.69, 140.44, 139.88, 126.81, 125.50, 122.76, 122.07, 119.23, 113.40, 111.05, 109.35, 104.18.

4.2.4 *3-chloro-1H-carbazole-1,4(9H)-dione* (**5**)

A solution of Fremy's Salt (1.4430g) and potassium dihydrogen orthophosphate (84.5mg) in water (85mL) was added to a solution of intermediate **4** (410mg, 1.88mmol) in acetone (85mL) at room temperature. The reaction mixture was stirred at at room temperature for 1.5 h and then evaporated under vacuum. The resulting precipitate was filtered, washed well with water and dried. A dark purple powder was obtained (413.3mg, 94.7%). m.p.: 263-265 °C. ^{1}H NMR (400 MHz, DMSO-d_6): δ 13.11 (s, 1H, NH), 8.05 (d, J = 8 Hz, 1H, ArH), 7.57 (d, J = 8 Hz, 1H, ArH), 7.43 (td, J = 0.96 Hz J = 8 Hz, 1H, ArH), 7.37 (td, J = 0.96 Hz J = 8 Hz, 1H, ArH), 7.18 (s, 1H,

ArH).

4.2.5*N-(3-chloro-4-oxo-4,9-dihydro-1H-carbazol-1-ylidene)-4-methylbenzenesulfonamide* (**6**)

Intermediate **6** was synthesized using the method similar to that of intermediate **2** except intermediate **5** was used as a starting material. The title compound was obtained as a brown solid (132.8 mg) in yield of 69.0%. m.p.: 234-235 °C. ^{1}H NMR (400 MHz, DMSO-d_6): δ 12.87 (s, 1H, aromatic NH), 8.11 (s, 1H, ArH), 8.00 (m, 3H, ArH), 7.54 (d, J = 8 Hz, 3H, ArH), 7.41 (t, J = 8 Hz, 1H, ArH), 7.33 (t, J = 8 Hz, 1H, ArH), 2.46 (s, 3H, CH_3).

4.2.6*2-((4-hydroxy-1-(4-methylphenylsulfonamido)-9H-carbazol-3-yl)thio)acetic acid* (**7**)

The title compound (21 mg, 21.3% yield) was obtained as a beige solid with method similar to M100 except intermediate **6** was used as a starting material. m.p.: 193-195 °C. ^{1}H NMR (400 MHz, DMSO-d_6): δ 13.33 (br s, 1H, COOH), 11.06 (s, 1H, aromatic NH), 9.48 (s, 1H, SO_2NH), 8.17 (d, J = 8 Hz, 1H, ArH), 7.57-7.51 (m, 3H, ArH), 7.34-7.30 (m, 3H, ArH), 7.14 (t, J = 8 Hz, 1H, ArH), 6.65 (s, 1H, ArH), 3.13 (s, 2H, CH_2), 2.36 (s, 3H, CH_3).^{13}C NMR (100 MHz, DMSO-d_6) δ 172.23, 153.62, 143.58, 139.61, 139.44, 136.81, 130.76, 129.88, 127.67, 125.57, 122.51, 122.21, 119.79, 113.36, 112.68, 111.69, 106.30, 21.44. ESI-MS ($C_{21}H_{18}N_2O_5S_2$): m/z 441.0593 (M-H$^+$); HRMS (ESI$^-$) m/z calculated for $C_{21}H_{17}N_2O_5S_2$ (M-H)$^-$: 441.05789, found 441.05734.

4.2.7 *ethyl 2-(4-amino-3-nitrophenoxy)acetate* (**9**)

A 100 mL 2-neck flask fitted with a stir-bar and an Ar inlet was charged with phenol **8** (4.9952 g, 32.4 mmol), K_2CO_3 (4.9346 g, 35.6 mmol) and acetone (60 mL), to which was added with ethyl bromoacetate (3.8 mL, 34.0 mmol) dropwise. The mixture was stirred at room temperature overnight. Salts were filtered through a pad of celite. The organic phase was concentrated to give solid which was triturated and

washed with PE/EtOAc=3/1 (50 mL) to remove red impurities and dried under infrared oven to obtain a yellow solid (5.8554 g, 75.2%). m.p.: 200-201 °C. ^{1}H NMR (400 MHz, DMSO-d_6): δ 7.37 (d, J = 2.24 Hz, 1H, ArH), 7.27 (s, 2H, NH_2), 7.22 (dd, J = 2.68 Hz J = 9.24 Hz, 1H, ArH), 7.01 (d, J = 9.24 Hz, 1H, ArH), 4.74 (s, 2H, OC$\underline{H}_2$CO), 4.17 (q, J = 7.08 Hz, 2H, COC$\underline{H}_2$CH$_3$), 1.21 (t, J = 7.12 Hz, 3H, CH$_2$C$\underline{H}_3$). ^{13}C NMR (100 MHz, DMSO-d_6): δ 169.09, 147.86, 142.71, 129.45, 127.71, 121.18, 107.47, 65.97, 61.11, 14.50.

4.2.8 *ethyl 2-((8-nitro-2,3,4,9-tetrahydro-1H-carbazol-6-yl)oxy)acetate* (**11**)

A suspension of **9** (5.8554 g, 24.4 mmol) in conc. HCl (40 mL) was cooled to -10 °C, to which was added a solution of $NaNO_2$ (2.027 g, 29.28 mmol) in water (3 mL) dropwise. After stirred for 0.5 h, a solution of $SnCl_2$ (11.04 g, 48.8 mmol) in conc. HCl (10 mL) was added slowly, and the mixture was stirred overnight and was used directly in the next step.

The phenylhydrazine **10** in conc. HCl was diluted with EtOH (50 mL). To this solution, cyclohexanone (2.5 mL, 24.4 mmol) was added dropwise. The mixture was heated to reflux for 3 hours. The acquired orange solid was filtered, washed with water (10 mL) twice and dried under infrared oven to give a red solid (3.2376 g, 41.7%). m.p.: 130-131 °C. ^{1}H NMR (400 MHz, $CDCl_3$): δ 9.34 (s, 1H, indole NH), 7.66 (s, 1H, ArH), 7.38 (s, 1H, ArH), 4.72 (s, 2H, OC$\underline{H}_2$CO), 4.32 (q, J = 7.12 Hz, 2H, COC$\underline{H}_2$CH$_3$), 2.79 (t, 2H, 1-CH$_2$), 2.67 (t, 2H, 4-CH$_2$), 1.93 (m, 4H, 2,3-CH$_2$CH$_2$) 1.34 (t, J = 7.08 Hz, 3H, CH$_2$C$\underline{H}_3$).^{13}C NMR (100 MHz, $CDCl_3$): δ 168.83, 150.81, 138.51, 132.31, 131.41, 125.74, 112.82, 111.13, 105.03, 66.90, 61.45, 23.17, 22.86, 22.80, 20.56, 14.18.

4.2.9 *ethyl 2-((1-nitro-9H-carbazol-3-yl)oxy)acetate* (**12**)

A suspension of **11** (3.2376 g, 10.17 mmol) and DDQ (5.54 g, 24.41 mmol) in toluene (50 mL) was refluxed at 110 °C for 2 hours. The mixture was diluted with EtOAc (100 mL), washed with saturated aqueous $NaHCO_3$ (100 mL) for five times till aqueous phase turned colorless. The organic phase was separated, dried over

anhydrous Na_2SO_4 and concentrated to afford a reddish brown solid (3.4166 g, quantitative). m.p.: 134-136 °C. ^{1}H NMR (400 MHz, DMSO-d_6): δ 11.97 (s, 1H, NH), 8.37 (s, 1H, ArH), 8.23 (d, J = 7.76 Hz, 1H, ArH), 7.86 (s, 1H, ArH), 7.71 (d, J = 8.16 Hz, 1H, ArH), 7.51 (t, 1H, ArH), 7.27 (t, 1H, ArH), 4.98 (s, 2H, OC$\underline{H}_2$CO), 4.21 (q, J = 7.08 Hz, 2H, COC$\underline{H}_2$CH$_3$), 1.24 (t, J = 7.16 Hz, 3H, CH$_2$C$\underline{H}_3$). ^{13}C NMR (100 MHz, DMSO-d_6): δ 169.15, 150.61, 141.93, 131.35, 129.40, 128.26, 128.06, 121.81, 121.46, 120.69, 116.03, 113.05, 108.62, 66.58, 61.18, 14.51.

4.2.10 *2-((1-nitro-9H-carbazol-3-yl)oxy)acetic acid* (**13**)

Ester **12** (1.255g, 4 mmol) was dissolved in THF (12 mL), and then a solution of LiOH (338.6 mg, 8 mmol) in water (12 mL) was added dropwise. The mixture was stirred at room temperature for 4.5 h. The mixture was diluted with EtOAc (80 mL), extracted with saturated aqueous $NaHCO_3$ (80 mL) for 3 times. The combined aqueous phase was acidified with 10% HCl until pH = 1. The yellow precipitate (1.1402 g, 99.8%) was collected by filtration and dried under infrared oven. m.p.: 180-181 °C. ^{1}H NMR (400 MHz, DMSO-d_6): δ 13.11 (br s, 1H, COOH), 11.97 (s, 1H, NH), 8.37 (s, 1H, ArH), 8.24 (d, J = 7.68 Hz, 1H, ArH), 7.85 (s, 1H, ArH), 7.71 (d, J = 8.04 Hz, 1H, ArH), 7.51 (t, 1H, ArH), 7.27 (t, 1H, ArH), 4.89 (s, 2H, C$\underline{H}_2$COOH). ^{13}C NMR (100 MHz, DMSO-d_6): δ 170.65, 150.84, 141.93, 131.37, 129.31, 128.24, 128.05, 121.82, 121.48, 120.68, 115.95, 113.04, 108.46, 66.35.

4.2.11 *3-methyl-5-(((1-nitro-9H-carbazol-3-yl)oxy)methyl)-1,2,4-oxadiazole* (**14**)

Acid **13** (167.0 mg, 0.58 mmol), HOBt (95.7 mg, 0.7 mmol) and EDCI (129.6 mg, 0.67 mmol) were slurried in dry acetonitrile (2 mL). The mixture was stirred at room temperature for 0.5 h. Methylamidoxime (57.3 mg, 0.61 mmol) in dry MeCN (1.5 mL) was added, then the mixture was refluxed overnight. After completion the mixture was concentrated and purified with flash column chromatography (PE/EtOAc = 3/1 as mobile phase) to afford an orange solid (101.8 mg, 53.8%). m.p.: 147-149 °C. ^{1}H NMR (400 MHz, DMSO-d_6): δ 12.04 (s, 1H, NH), 8.49 (d, J = 1.68 Hz, 1H, ArH), 8.24 (d, J = 7.80 Hz, 1H, ArH), 8.01 (d, J = 1.68 Hz, 1H, ArH), 7.72 (d, J = 8.16 Hz,

1H, ArH), 7.52 (t, 1H, ArH), 7.28 (t, 1H, ArH), 5.70 (s, 2H, OCH_2), 2.38 (s, 3H, CH_3). ^{13}C NMR (100 MHz, $CDCl_3$): δ 174.09, 167.61, 150.33, 140.60, 131.25, 130.04, 128.23, 128.20, 121.76, 121.09, 120.79, 115.47, 111.72, 108.31, 62.55, 11.56.

4.2.12 *2-methyl-5-(((1-nitro-9H-carbazol-3-yl)oxy)methyl)-1,3,4-oxadiazole* (**15**)

Acid **13** (561.7 mg, 1.96 mmol), acetohydrazide (291.4 mg, 4 mmol), HOBt (400.6 mg, 3 mmol) and EDCI (565.4 mg, 3 mmol) were combined in DMF (8 mL). The mixture was stirred at room temperature for 12 hours. Then the solution was diluted with water (50 mL). Red precipitate was filtered, washed with water (10 mL) for 3 times and dried. The red solid (502.0 mg, 74.7%) was used directly in the next step.

The red solid obtained (173.2 mg, 0.5 mmol) was dissolved in $POCl_3$ (2 mL) in a sealed tube which was then, heated to 100 °C for 1 h. Then the mixture was poured into cold water, neutralized with saturated $NaHCO_3$ solution (pH = 12) and extracted with DCM (50 mL) twice. The combined DCM solution was dried with anhydrous Na_2SO_4, concentrated and the crude solid was triturated in DCM/PE=1/1. The acquired orange solid was filtered and washed with DCM/PE=1/1 to afford pure product (107.9 mg, 65.8%). m.p.: 163-164 °C. ^1H NMR (400 MHz, DMSO-d_6): δ 12.02 (s, 1H, NH), 8.47 (s, 1H, ArH), 8.23 (d, J = 7.76 Hz, 1H, ArH), 8.02 (s, 1H, ArH), 7.72 (d, J = 8.08 Hz, 1H, ArH), 7.52 (t, 1H, ArH), 7.28 (t, 1H, ArH), 5.57 (s, 2H, CH_2), 2.55 (s, 3H, CH_3). ^{13}C NMR (100 MHz, DMSO-d_6): δ 165.30, 162.78, 150.18, 141.98, 131.40, 129.69, 128.33, 128.19, 121.78, 121.46, 120.80, 116.53, 113.11, 108.95, 61.49, 10.97.

4.2.13 *8-nitro-2,3,4,9-tetrahydro-1H-carbazol-6-ol* (**18**)

A suspension of aniline **16** (4.6192 g, 30 mmol) in conc. HCl (50 mL) was stirred at room temperature for 0.5 h till black solid turned into white suspension then cooled to -10 °C, to which a solution of $NaNO_2$ (2.4897 g, 36 mmol) in water (3.5 mL) was added dropwise. After stirred for 1 h, a solution of $SnCl_2$ (13.6 g, 60 mmol) in conc. HCl (10 mL) was added slowly. After completion the mixture was stirred at -10 °C for

1h, followed by stirr at room temperature for another 3 hours. The mixture was used directed in the next step.

The phenylhydrazine **17** solution in conc. HCl was diluted with EtOH (50 mL), to which was added dropwise with cyclohexanone (3.4 mL, 33 mmol). The mixture was heated and refluxed overnight. Black solid was filtered, washed with water (10 mL) twice and dried under infrared oven to give a black solid (2.3455 g, 38.1%). m.p.: 205-206 °C. ^{1}H NMR (400 MHz, DMSO-d_6): δ 11.19 (s, 1H, NH), 9.44 (s, 1H, OH), 7.43 (s, 1H, ArH), 7.22 (s, 1H, ArH), 2.74 (t, 2H, 1-CH_2), 2.58 (t, 2H, 4-CH_2), 1.80 (m, 4H, 2, 3-CH_2). ^{13}C NMR (100 MHz, DMSO-d_6): δ 149.91, 139.70, 132.79, 131.49, 124.07, 112.58, 109.62, 104.86, 23.40, 23.07, 23.00, 20.69.

4.2.14 *8-nitro-2,3,4,9-tetrahydro-1H-carbazol-6-yl trifluoromethanesulfonate* (**19**)

To a suspension of **18** (116.6 mg, 0.5 mmol) in DCM (5 mL), 2,6-Lutidine (64 uL, 0.55 mmol) was added dropwise in an ice bath. Subsequently, Tf_2O (68.9 uL, 0.55 mmol) was added over 5 min. The mixture was stirred overnight. Then, another portion of 2,6-Lutidine (128 uL, 1.1 mmol) and Tf_2O (68.9 uL, 0.55 mmol) was added, and the mixture was stirred for another 5.5 hours. After completion, the mixture was diluted with DCM (20 mL), washed with 2N HCl (20 mL) twice, brine (20 mL), dried over anhydrous Na_2SO_4 and concentrated to afford a yellow solid (181.7 mg, 99.3%). m.p.: 133-135 °C. ^{1}H NMR (400 MHz, DMSO-d_6): δ 11.93 (s, 1H, NH), 7.98 (s, 2H, ArH), 2.80 (t, 2H, 1-CH_2), 2.66 (t, 2H, 4-CH_2), 1.82 (m, 4H, 2, 3-CH_2). ^{13}C NMR (100 MHz, DMSO-d_6): δ 142.41, 140.63, 132.47, 131.23, 127.63, 118.78 (q, J = 320 Hz), 118.10, 111.63, 110.00, 23.42, 22.77, 22.71, 20.55.

4.2.15 *1-nitro-9H-carbazol-3-yl trifluoromethanesulfonate* (**20**)

A suspension of **19** (181.7 mg, 0.5 mmol) and DDQ (272.4 mg, 1.2 mmol) in toluene (5 mL) was refluxed at 110 °C overnight. The mixture was diluted with EtOAc (50 mL), washed with saturated aqueous $NaHCO_3$ (50 mL) for 5 times till aqueous phase turned colorless. The organic phase was separated, dried over anhydrous Na_2SO_4 and concentrated. The crude product was purified by flash column

chromatography (DCM/PE=1/3) to afford a yellow solid (126.5 mg, 77.5%). m.p: 142-144 °C. ^{1}H NMR (400 MHz, DMSO-d_6): δ 12.46 (s, 1H, NH), 8.89 (s, 1H, ArH), 8.37 (s, 2H, ArH), 7.78 (d, 1H, ArH), 7.59 (t, 1H, ArH), 7.35 (t, 1H, ArH).^{13}C NMR (100 MHz, DMSO-d_6): δ 142.16, 140.37, 132.47, 131.24, 129.04, 128.47, 121.93, 121.65, 121.57, 121.45, 118.81 (q, J = 320 Hz), 114.87, 113.47. ^{19}F NMR (376 MHz, DMSO-d_6): δ -72.41.

4.2.16 *ethyl 2-((1-nitro-9H-carbazol-3-yl)thio)acetate* (**21**)

$Pd_2(dba)_3$ (2311.4 mg, 0.25 mmol) and xantphos (292.4 mg, 0.5 mmol) were premixed in dioxane (4 mL) under Ar_2 for 1 hour. Intermediate **20** (360 mg, 1 mmol) was added subsequently, the reaction mixture was backfilled with Ar_2 (2 cycles). Then DIPEA (0.35 mL) and ethyl mercaptoacetate (0.11 mL) were added. The mixture was refluxed overnight (20 hours). After completion, the mixture was diluted with EtOAc (50 mL), filtered through a pad of celite to remove catalyst, washed with 2N HCl (50 mL) for 3 times, dried over anhydrous Na_2SO_4 and concentrated. The crude product was purified by flash column chromatography (EtOAc/PE = 1/20 to 1/10) to afford a yellow solid (250.0 mg, 75.6%). m.p.: 134-135 °C. ^{1}H NMR (400 MHz, DMSO-d_6): δ 12.25 (s, 1H, carbazole NH), 8.76 (s, 1H, ArH), 8.35 (s, 1H, ArH), 8.27 (d, J = 7.76 Hz, 1H, ArH), 7.75 (d, J = 8.12 Hz, 1H, ArH), 7.54 (t, 1H, ArH), 7.32 (t, 1H, ArH), 4.07 (q, J = 7.12 Hz, 2H, $C\underline{H}_2CH_3$), 3.93 (s, 2H, $SC\underline{H}_2$), 1.10 (t, J = 7.08 Hz, 3H, $CH_2C\underline{H}_3$).^{13}C NMR (100 MHz, DMSO-d_6): δ 169.75, 141.58, 132.83, 131.95, 131.59, 128.42, 128.30, 124.83, 123.72, 121.48, 121.42, 113.22, 61.35, 37.72, 14.38.

4.2.17 *ethyl 2-((1-(4-methylphenylsulfonamido)-9H-carbazol-3-yl)oxy)acetate* (**22a**)

To a suspension of **12** (315.1 mg, 1 mmol) in MeOH (25 mL), Pd/C (10%, 65.7 mg) was added. The mixture was stirred in a hydrogen generator (40 psi, room temperature) overnight. The suspension was filtered through a pad of celite, and the filtrate was concentrated under reduced pressure. The crude product was used in the next step without further purification.

To a solution of the obtained aniline in pyridine (10 mL), TsCl (263.1 mg, 1.38

mmol) was added portionwise. The mixture was stirred at toom temperature for 24 hs before pyridine was removed under reduced pressure. The crude product was purified by flash column chromatography (PE/Acetone = 3/1) to afford a white solid (221.1 mg, 50.4%). m.p.: 145-147 °C. ^{1}H NMR (400 MHz, DMSO-d_6): δ 10.75 (s, 1H, carbazoleNH), 10.00 (s, 1H, $NHSO_2$), 8.02 (d, J = 7.80 Hz, 1H, ArH), 7.68 (d, J = 8.24 Hz, 2H, ArH), 7.54 (d, J = 8.16 Hz, 1H, ArH), 7.49 (d, J = 2.24 Hz, 1H, ArH), 7.37 (td, 1H, ArH), 7.33 (d, J = 8.08 Hz, 2H, ArH), 7.12 (t, 1H, ArH), 6.68 (d, J = 2.32 Hz, 1H, ArH), 4.70 (s, 2H, $OC\underline{H}_2CO$), 4.17 (q, J = 7.12 Hz, 2H, $COC\underline{H}_2CH_3$), 2.32 (s, 3H, $PhC\underline{H}_3$), 1.22 (t, J = 7.08 Hz, 3H, $CH_2C\underline{H}_3$).^{13}C NMR (100 MHz, DMSO-d_6): δ 169.32, 151.55, 143.85, 140.43, 137.08, 130.11, 129.43, 127.34, 126.36, 124.27, 122.71, 121.93, 120.78, 119.00, 112.02, 109.07, 102.06, 66.16, 61.00, 21.40, 14.51.ESI-MS ($C_{23}H_{22}N_2O_5S$): m/z 437.1193 ($M\text{-}H^+$);HRMS (ESI^-) m/z calculated for $C_{23}H_{21}N_2O_5S^-$ $(M\text{-}H)^-$: 437.11712, found 437.11767.

4.2.18 *ethyl 2-((1-(4-acetamidophenylsulfonamido)-9H-carbazol-3-yl)oxy)acetate* (**22b**)

The title compound (103.9 mg, 21.6%) was obtained as a white solid using a method similar to that of **22a** except 4-acetamidophenylsulfonyl chloride was used as the starting material. m.p.: 227-228 °C. ^{1}H NMR (400 MHz, DMSO-d_6): δ 10.73 (s, 1H, carbazole NH), 10.26 (s, 1H, $N\underline{H}COCH_3$), 9.93 (s, 1H, $NHSO_2$), 8.02 (d, J = 7.76 Hz, 1H, ArH), 7.70 (m, 4H, ArH), 7.54 (d, J = 8.12 Hz, 1H, ArH), 7.49 (s, 1H, ArH), 7.37 (t, 1H, ArH), 7.12 (t, 1H, ArH), 6.68 (s, 1H, ArH), 4.71 (s, 2H, OCH_2CO), 4.17 (q, J = 7.08 Hz, 2H, $COC\underline{H}_2CH_3$), 2.04 (s, 3H, $NHCOC\underline{H}_3$), 1.22 (t, J = 7.08 Hz, 3H, $CH_2C\underline{H}_3$). ^{13}C NMR (100 MHz, DMSO-d_6): δ 169.45, 169.34, 151.55, 143.70, 140.44, 133.34, 129.53, 128.56, 126.35, 124.26, 122.71, 121.95, 120.77, 118.98, 118.90, 112.02, 109.25, 102.06, 66.15, 60.99, 24.56, 14.51. ESI-MS ($C_{24}H_{23}N_3O_6S$): m/z 480.1262 ($M\text{-}H^+$); HRMS (ESI^-) m/z calculated for $C_{24}H_{22}N_3O_6S^-$ $(M\text{-}H)^-$: 480.12293, found 480.12348.

4.2.19

4-methyl-N-(3-((3-methyl-1,2,4-oxadiazol-5-yl)methoxy)-9H-carbazol-1-yl)benzenesulfonamide (**22c**)

A solution of **14** (153.7 mg, 0.474 mmol) in DCM/MeOH (15 mL/15 mL) was added with a solution of $Na_2S_2O_4$ (1.03 g, 5.688 mmol) and K_2CO_3 (814.0 mg, 5.688 mmol) in water (4 mL) over 30 min. The mixture was stirred at room temperature under Ar_2 for 2 hours. Then, the inorganic salts were filtered off, and the filtrate was concentrated and used directly in the next step.

To a solution of the obtained aniline in pyridine (10 mL), TsCl (128.8 mg, 0.65 mmol) was added portionwise. The mixture was stirred at room temperature for 19 hours. Another portion of TsCl (91.9 mg) was added, and the mixture was stirred for another 3 hours before pyridine was removed under reduced pressure. The crude product was purified by flash column chromatography (PE/Acetone=3/1) to afford a white solid (29.2 mg, 13.7%).m.p.: 162-163 °C. ^{1}H NMR (400 MHz, DMSO-d_6): δ 10.79 (s, 1H, carbazoleNH), 10.02 (s, 1H, $NHSO_2$), 8.02 (d, J = 7.76 Hz, 1H, ArH), 7.67 (d, J = 8.12 Hz, 2H, ArH), 7.65 (s, 1H, ArH), 7.55 (d, J = 8.24 Hz, 1H, ArH), 7.38 (t, 1H, ArH), 7.32 (d, J = 7.96 Hz, 2H, ArH), 7.13 (t, 1H, ArH), 6.75 (s, 1H, ArH), 5.42 (s, 2H, CH_2), 2.36 (s, 3H, oxadiazole C$\underline{H}_3$), 2.31 (s, 3H, PhC$\underline{H}_3$).^{13}C NMR (100 MHz, DMSO-d_6): δ 175.59, 167.51, 151.20, 143.90, 140.45, 136.99, 130.12, 129.67, 127.34, 126.49, 124.27, 122.67, 122.09, 120.78, 119.13, 112.09, 109.21, 102.48, 62.19, 21.41, 11.55. HRMS (ESI^-) m/z calculated for $C_{23}H_{19}N_4O_4S^-$ $(M-H)^-$: 447.11270, found 447.11215.

4.2.20

4-methyl-N-(3-((5-methyl-1,3,4-oxadiazol-2-yl)methoxy)-9H-carbazol-1-yl)benzenesulfonamide (**22d**)

The title compound (34.6 mg, 27.4%) was obtained as a white solid using a method similar to that of **22a** except **15** was used as starting material. mp：179-180 °C. ^{1}H NMR (400 MHz, DMSO-d_6): δ 10.77 (s, 1H, carbazole NH), 10.13 (s, 1H, $NHSO_2$), 8.02 (d, J = 7.52 Hz, 1H, ArH), 7.68 (d, J = 7.52 Hz, 2H, ArH), 7.62 (s, 1H, ArH), 7.55 (d, J = 7.96 Hz, 1H, ArH), 7.37 (t, 1H, ArH), 7.31 (d, J = 7.52 Hz, 2H,

ArH), 7.13 (t, 1H, ArH), 6.77 (s, 1H, ArH), 5.30 (s, 2H, CH_2), 2.53 (s, 3H, oxadiazole C$\underline{H}_3$), 2.30 (s, 3H, PhC$\underline{H}_3$). ^{13}C NMR (100 MHz, DMSO-d_6): δ 165.13, 163.08, 151.31, 143.56, 140.39, 137.55, 130.03, 129.74, 127.30, 126.33, 124.05, 123.12, 122.76, 120.70, 119.02, 112.07, 108.98, 101.97, 61.14, 21.38, 10.96. HRMS (ESI^-) m/z calculated for $C_{23}H_{19}N_4O_4S^-$ $(M-H)^-$: 447.11270, found 447.11215.

4.2.21

N-(4-(N-(3-((5-methyl-1,3,4-oxadiazol-2-yl)methoxy)-9H-carbazol-1-yl)sulfamoyl)phenyl)acetamide (**22e**)

The title compound (182 mg, 52.7%) was obtained as a white solid using a method similar to that of **22a** except **15** and 4-acetamidophenylsulfonyl chloride were used as starting materials. m.p.: 224-226 °C. ^{1}H NMR (400 MHz, DMSO-d_6): δ 10.78 (s, 1H, carbazole NH), 10.26 (s, 1H, N$\underline{H}$COCH$_3$), 9.97 (s, 1H, SO_2NH), 8.03 (d, J = 7.84 Hz, 1H, ArH), 7.73-7.67 (m, 5H, ArH), 7.55 (d, J = 8.20 Hz, 1H, ArH), 7.38 (td, 1H, ArH), 7.14 (td, 1H, ArH), 6.75 (d, J = 2.32 Hz, 1H, ArH), 5.31 (s, 2H, CH_2), 2.53 (s, 3H, oxadiazole CH_3), 2.04 (s, 3H, NHCOC$\underline{H}_3$). ^{13}C NMR (100 MHz, DMSO-d_6): δ 169.46, 165.15, 163.04, 151.21, 143.71, 140.45, 133.28, 129.75, 128.58, 126.46, 124.26, 122.69, 122.10, 120.76, 119.12, 118.94, 112.08, 109.54, 102.75, 61.21, 24.56, 10.95. HRMS (ESI^+) m/z calculated for $C_{24}H_{22}N_5O_5S^+$ $(M+H)^+$: 492.13362, found 492.13362; calculated for $C_{24}H_{21}N_5O_5SK^+$ $(M + K^+)$: 530.08950, found 530.09093.

4.2.22

N-(3-(N-(3-((5-methyl-1,3,4-oxadiazol-2-yl)methoxy)-9H-carbazol-1-yl)sulfamoyl)phenyl)acetamide (**22f**)

The title compound (122.5 mg, 54%) was obtained as a white solid using a method similar to that of **22a** except **15** and 3-acetamidophenylsulfonyl chloride were used as starting materials. m.p.: 210-212 °C. ^{1}H NMR (400 MHz, DMSO-d_6): δ 10.80 (s, 1H, carbazole N$\underline{H}$), 10.23 (s, 1H, N$\underline{H}$COCH$_3$), 10.18 (s, 1H, SO_2N$\underline{H}$), 8.27 (s, 1H, ArH), 8.04 (d, J = 7.84 Hz, 1H, ArH), 7.70-7.67 (m, 2H, ArH), 7.56 (d, J = 8.16 Hz, 1H, ArH), 7.45 (d, J = 4.80 Hz, 2H, ArH), 7.39 (t, 1H, ArH), 7.14 (t, 1H, ArH), 6.74

(d, *J* = 2.04 Hz, 1H, ArH), 5.31 (s, 2H, CH_2), 2.53 (s, 3H, oxadiazole CH_3), 2.04 (s, 3H, NHCOC<u>H</u>$_3$). ^{13}C NMR (100 MHz, DMSO-d_6): δ 169.29, 165.17, 163.02, 151.20, 140.47, 140.36, 140.32, 130.10, 129.88, 126.50, 124.30, 123.28, 122.66, 121.82, 121.63, 120.78, 119.13, 117.36, 112.09, 109.74, 102.87, 61.15, 24.47, 10.96. HRMS (ESI^-) m/z calculated for $C_{24}H_{20}N_5O_5S^-$ (M-H) $^-$490.11851, found 490.11906.

4.2.23 *ethyl 2-((1-(4-methylphenylsulfonamido)-9H-carbazol-3-yl)thio)acetate* (**22g**)

The title compound (122.5 mg, 54%) was obtained as a white solid using a method similar to that of **22c** except **21** and TsCl were used as starting materials. m.p.: 150-151 °C. ^{1}H NMR (400 MHz, DMSO-d_6): δ 11.10 (s, 1H, carbazoleNH), 9.94 (s, 1H, SO_2NH), 8.09 (d, *J* = 8.20 Hz, 1H, ArH), 8.07 (s, 1H, ArH), 7.64 (d, *J* = 7.96 Hz, 2H, ArH), 7.59 (d, *J* = 8.12 Hz, 1H, ArH), 7.42 (t, 1H, ArH), 7.33 (d, *J* = 7.84 Hz, 2H, ArH), 7.18 (t, 1H, ArH), 7.00 (s, 1H, ArH), 4.03 (q, *J* = 7.08 Hz, 2H, C<u>H</u>$_2$CH$_3$), 3.58 (s, 2H, SCH_2), 2.33 (s, 3H, PhC<u>H</u>$_3$), 1.09 (t, *J* = 7.12 Hz, 3H, CH_2C<u>H</u>$_3$).^{13}C NMR (100 MHz, DMSO-d_6): δ 169.69, 143.84, 140.31, 136.85, 134.70, 130.03, 127.45, 126.81, 124.97, 124.29, 123.03, 122.52, 122.18, 121.76, 120.87, 119.78, 112.17, 61.15, 38.56, 21.40, 14.40. HRMS (ESI^-) m/z calculated for $C_{23}H_{21}N_2O_4S_2^-$ $(M-H)^-$: 453.09427; found 453.09482.

4.2.24 *ethyl 2-((1-(4-acetamidophenylsulfonamido)-9H-carbazol-3-yl)thio)acetate* (**22h**)

The title compound (186 mg, 49.4%) was obtained as a white solid using a method similar to that of **22c** except **21** and 4-acetamidophenylsulfonyl chloride were used as starting materials. m.p.: 225-226 °C. ^{1}H NMR (400 MHz, DMSO-d_6): δ 11.09 (s, 1H, carbazole NH), 10.26 (s, 1H, N<u>H</u>COCH$_3$), 9.89 (s, 1H, SO_2NH), 8.09 (d, *J* = 8.08 Hz, 1H, ArH), 8.07 (s, 1H, ArH), 7.69 (t, 4H, ArH), 7.59 (d, *J* = 8.08 Hz, 1H, ArH), 7.42 (t, 1H, ArH), 7.18 (t, 1H, ArH), 7.03 (s, 1H, ArH), 4.02 (q, *J* = 7.04 Hz, 2H, C<u>H</u>$_2$CH$_3$), 3.59 (s, 2H, SCH_2), 2.05 (s, 3H, NHCOC<u>H</u>$_3$), 1.07 (t, *J* = 7.04 Hz, CH_2C<u>H</u>$_3$). ^{13}C NMR (100 MHz, DMSO-d_6): δ 169.72, 169.43, 143.73, 140.30, 134.75, 133.16, 128.63, 126.80, 124.96, 124.43, 122.98, 122.57, 122.19, 121.80, 120.86,

119.77, 118.86, 112.16, 61.13, 38.58, 24.57, 14.39. HRMS (ESI$^-$) m/z calculated for $C_{24}H_{22}N_3O_5S_2^-$ (M-H) $^-$: 496.10009, found 496.10064.

4.2.25 *2-((1-(4-methylphenylsulfonamido)-9H-carbazol-3-yl)thio)acetic acid* (**22i**)

The solution of **22g** (89.5 mg, 0.2mmol) in THF (1 mL) was added with aquaous NaOH solution (1 N, 1 mL) dropwise. The mixture was stirred at room temperature for 0.5 hour before diluted with EtOAc (20 mL) and extracted with saturated aqueous $NaHCO_3$ (20 mL) for 3 times. Aqueous phase was acidified with 2N HCl till pH = 1 to allow white solid to precipitate. White precipitate (74.2 mg, 88.4%) was collected by filtration and dried under infrared oven. m.p.: 192-193 °C. ^{1}H NMR (400 MHz, DMSO-d_6): δ 12.51 (s, 1H, COOH), 11.10 (s, 1H, carbazole NH), 10.03 (s, 1H, SO_2NH), 8.08 (d, *J* = 7.96 Hz, 1H, ArH), 8.05 (s, 1H, ArH), 7.65 (d, *J* = 7.96 Hz, 2H, ArH), 7.58 (d, *J* = 7.96 Hz, 1H, ArH), 7.41 (t, 1H, ArH), 7.32 (d, *J* = 7.96 Hz, 2H, ArH), 7.18 (t, 1H, ArH), 7.01 (s, 1H, ArH), 3.55 (s, 2H, SCH_2), 2.32 (s, 3H, PhC$\underline{H}_3$). ^{13}C NMR (100 MHz, DMSO-d_6): δ 171.06, 143.85, 140.29, 136.82, 134.46, 130.04, 127.47, 126.76, 124.96, 123.80, 123.75, 122.18, 121.79, 121.72, 120.87, 119.70, 112.14, 38.85, 21.42. HRMS (ESI$^-$) m/z calculated for $C_{21}H_{17}N_2O_4S_2^-$ (M-H)$^-$: 425.06297, found 425.06352.

4.2.26 *2-((1-(4-acetamidophenylsulfonamido)-9H-carbazol-3-yl)thio)acetic acid* (**22j**)

The title compound (65.8 mg, 82.3%) was obtained as a white solid using a method similar to that of **22i** except **22h** was used as starting material. m.p.: 145-146 °C. ^{1}H NMR (400 MHz, DMSO-d_6): δ 12.23 (br s, 1H, COOH), 11.09 (s, 1H, carbazole NH), 10.26 (s, 1H, N$\underline{H}$COCH$_3$), 9.97 (br s, 1H, SO_2NH), 8.08 (d, *J* = 8.00 Hz, 1H, ArH), 8.05 (s, 1H, ArH), 7.69 (s, 4H, ArH), 7.58 (d, *J* = 7.92 Hz, 1H, ArH), 7.41 (t, 1H, ArH), 7.17 (t, 1H, ArH), 7.03 (s, 1H, ArH), 3.56 (s, 2H, ArH), 2.05 (s, 3H, ArH). ^{13}C NMR (100 MHz, DMSO-d_6): δ 171.11, 169.45, 143.70, 140.28, 134.47, 133.20, 128.66, 126.74, 124.95, 123.84, 123.80, 122.18, 121.83, 121.66, 120.87, 119.69, 118.90, 112.13, 38.92, 24.57. HRMS (ESI$^-$) m/z calculated for $C_{22}H_{18}N_3O_5S_2^-$ (M-H) $^-$: 468.06879, found 468.06934.

4.2.27 *2-((1-(4-methylphenylsulfonamido)-9H-carbazol-3-yl)oxy)acetic acid* (**22k**)

The title compound (58.0 mg, 81%) was obtained as a white solid by using a method similar to that of **22i** except **22a** was used as the starting material. m.p.: 186-188 °C. ^{1}H NMR (400 MHz, DMSO-d_6): δ 12.96 (br s, 1H, COOH), 10.75 (s, 1H, carbazole NH), 10.02 (br s, 1H, $NHSO_2$), 8.02 (d, J = 7.80 Hz, 1H, ArH), 7.70 (d, J = 7.92 Hz, 2H, ArH), 7.54 (d, J = 8.12 Hz, 1H, ArH), 7.47 (s, 1H, ArH), 7.37 (t, 1H, ArH), 7.33 (d, J = 8.08 Hz, 2H, ArH), 7.11 (t, 1H, ArH), 6.70 (s, 1H, ArH), 4.61 (s, 2H, CH_2), 2.32 (s, 3H, CH_3). ^{13}C NMR (100 MHz, DMSO-d_6): δ 170.84, 151.74, 143.86, 140.42, 137.10, 130.12, 129.30, 127.36, 126.31, 124.24, 121.96, 120.76, 118.97, 112.00, 109.07, 101.75, 65.94, 21.41. HRMS (ESI$^-$) m/z calculated for $C_{21}H_{17}N_2O_5S^-$(M-H)$^-$: 409.08582, found 409.08637.

4.2.28 *2-((1-(4-methylphenylsulfonamido)-9H-carbazol-3-yl)oxy)acetamide* (**22l**)

22a (440 mg, 1 mmol) was dissolved in aqueous ammonia (25%, 18 mL) and was stirred at room temperature for 3 hours. After completion, ammonia and water was removed to afford a beige solid (389.9 mg, 94.9%). m.p.: 235-236 °C. ^{1}H NMR (400 MHz, DMSO-d_6): δ 10.74 (s, 1H, carbazole N<u>H</u>), 10.00 (s, 1H, SO_2N<u>H</u>), 8.01 (d, J = 7.76 Hz, 1H, ArH), 7.71 (d, J = 8.08 Hz, 2H, ArH), 7.54 (d, J = 8.08 Hz, 1H, ArH), 7.49 (d, J = 1.64 Hz, 1H, ArH), 7.41-7.31 (m, 4H, ArH), 7.12 (t, 1H, ArH), 6.84 (d, J = 1.84 Hz, 1H, ArH), 4.39 (s, 2H, CH_2), 2.30 (s, 3H, PhC<u>H</u>$_3$). ^{13}C NMR (100 MHz, DMSO-d_6): δ 170.57, 151.74, 143.87, 140.37, 137.05, 130.12, 129.19, 127.39, 126.33, 124.19, 122.72, 122.02, 120.70, 119.03, 112.02, 109.09, 101.85, 68.20, 21.41. HRMS (ESI$^-$) m/z calculated for $C_{21}H_{18}N_3O_4S^-$(M-H) $^-$: 408.10180, found 408.10235.

4.2.29

N-(3-((1H-tetrazol-5-yl)methoxy)-9H-carbazol-1-yl)-4-methylbenzenesulfonamide

(**22m**)

To a sealed tube, **22l** (271.8 mg, 0.66 mmol), NaN_3 (651.6 mg, 9.96 mmol), $SiCl_4$ (0.38 mL, 3.32 mmol) and dry MeCN (6 mL) were combined. The mixture was

heated to 80 °C for 14 hours and diluted with MeOH (50 mL) before inorganic salts were removed. The filtrate was concentrated and purified by column chromatography (silica gel, MeOH/DCM = 1/30 - 1/20) to give a white solid (179.2 mg, 62.1%). m.p.: 235-237 °C. ^{1}H NMR (400 MHz, DMSO-d_6): δ 10.79 (s, 1H, carbazole NH), 10.05 (s, 1H, SO_2NH), 8.04 (d, J = 7.80 Hz, 1H, ArH), 7.68 (d, 3H, ArH), 7.56 (d, J = 8.16 Hz, 1H, ArH), 7.38 (t, 1H, ArH), 7.31 (d, J = 8.08 Hz, 2H, ArH), 7.14 (t, 1H, ArH), 6.83 (d, J = 2.00 Hz, 1H, ArH), 5.46 (s, 2H, CH_2), 2.30 (s, 3H, PhCH_3). ^{13}C NMR (100 MHz, DMSO-d_6): δ 151.31, 143.91, 140.39, 136.96, 130.14, 129.41, 127.32, 126.47, 124.25, 122.69, 122.10, 120.77, 119.13, 112.09, 109.20, 102.31, 60.87, 21.41. HRMS (ESI^+) m/z calculated for $C_{21}H_{18}N_6O_3S^+$ M^+: 434.11556, found 434.11556; $C_{21}H_{18}N_6O_3SK^+$ ($M + K^+$): 473.07927, found 473.08103.

4.2.30

N-(3-(2-hydrazinyl-2-oxoethoxy)-9H-carbazol-1-yl)-4-methylbenzenesulfonamide (**22n**)

22a (943.4, 2.15 mmol) and hydrazine hydrate (1.05 mL, 50 wt%) were refluxed in EtOH (13 mL) until solid was dissolved. The solution was cooled to room temperature to generate white precipitate (758.2 mg, 83.0%) which was collected by filtration, washed with cold EtOH and dried in sequence. m.p.: 167-168 °C. ^{1}H NMR (400 MHz, DMSO-d_6): δ 10.73 (s, 1H, carbazole NH), 10.01 (s, 1H, SO_2NH), 9.39 (s, 1H, CONHNH_2), 8.01 (d, J = 7.72 Hz, 1H, ArH), 7.71 (d, J = 7.96 Hz, 2H, ArH), 7.54 (d, J = 8.12 Hz, 1H, ArH), 7.49 (s, 1H, ArH), 7.37 (t, 1H, ArH), 7.33 (d, J = 7.92 Hz, 2H, ArH), 7.12 (t, 1H, ArH), 6.84 (s, 1H, ArH), 4.45 (s, 2H, CH_2), 4.36 (s, 2H, CONHNH_2), 2.31 (s, 3H, PhCH_3). ^{13}C NMR (100 MHz, DMSO-d_6): δ 167.17, 151.81, 143.86, 140.35, 137.07, 130.13, 129.15, 127.38, 126.32, 124.14, 122.73, 122.02, 120.70, 119.01, 112.03, 109.22, 101.61, 67.72, 21.41.

4.2.31

N-(3-((5-amino-1,3,4-oxadiazol-2-yl)methoxy)-9H-carbazol-1-yl)-4-methylbenzenesulfonamide (**22o**)

To a suspension of **22n** (422.1 mg, 1 mmol) in EtOH (10 mL), BrCN (121.0 mg, 1.2 mmol) was added, and the mixture was refluxed for 3 hours before solvent was removed. The residue was purified by column chromatography (acetone / DCM = 1/4 - 1/2) to obtain a white solid (102 mg, 22.8%). m.p.: 157-158 °C. ^{1}H NMR (400 MHz, DMSO-d_6): δ 10.79 (s, 1H, carbazole N<u>H</u>), 10.02 (s, 1H, SO_2N<u>H</u>), 8.02 (d, J = 7.20 Hz, 1H, ArH), 7.68 (t, 3H, ArH), 7.55 (d, J = 7.64 Hz, 1H, ArH), 7.38 (t, 1H, ArH), 7.32 (d, J = 7.08 Hz, 2H, ArH), 7.20 (s, 2H, NH_2), 7.14 (t, 1H, ArH), 6.74 (s, 1H, ArH), 5.11 (s, 2H, CH_2), 2.30 (s, 3H, PhC<u>H</u>$_3$). ^{13}C NMR (100 MHz, DMSO-d_6): δ 164.90, 155.93, 151.26, 143.90, 140.41, 136.95, 130.14, 129.51, 127.37, 126.45, 124.26, 122.69, 122.05, 120.74, 119.11, 112.08, 109.34, 102.54, 61.17, 21.41. HRMS (ESI$^+$) m/z calculated for $C_{22}H_{20}N_5O_4S^+$(M+H)$^+$: 450.12305, found 450.12305; $C_{22}H_{19}N_5O_4SNa^+$ (M + Na^+): 472.10500, found 472.10488; $C_{22}H_{19}N_5O_4SK^+$ (M + K^+) 488.07893, found 488.07883.

4.2.32 *ethyl 2-((1-(4-methylphenylsulfonamido)-9H-carbazol-3-yl)sulfonyl)acetate* (**22p**)

To a solution of **22g** (100.3 mg, 0.22 mmol) in acetone (4 mL) was added an aqueous solution of oxone (700.4 mg, 1.1 mmol). The mixture was stirred at room temperature overnight before white suspension was filtered, washed with water and dried. The solid collected was purified by column chromatography (acetone/PE = 1/3) to obtain a white solid (52.7 mg, 49.3%). m.p.: 231-232 °C. ^{1}H NMR (400 MHz, DMSO-d_6): δ 11.66 (s, 1H, carbazole NH), 10.17 (s, 1H, SO_2NH), 8.55 (d, J = 1.52 Hz, 1H, ArH), 8.26 (d, J = 7.84 Hz, 1H, ArH), 7.68 (d, J = 8.20 Hz, 1H, ArH), 7.64 (d, J = 8.28 Hz, 2H, ArH), 7.52 (td, 1H, ArH), 7.37 (d, J = 1.64 Hz, 1H, ArH), 7.34 (d, J = 8.00 Hz, 2H, ArH), 7.29 (td, 1H, ArH), 4.35 (s, 2H, SO_2CH_2), 3.98 (q, J = 7.12 Hz, 2H, C<u>H</u>$_2$CH$_3$), 2.32 (s, 3H, PhC<u>H</u>$_3$), 0.97 (t, J = 7.12 Hz, 3H, CH_2C<u>H</u>$_3$). ^{13}C NMR (100 MHz, DMSO-d_6): δ 162.96, 144.09, 140.79, 137.98, 136.45, 130.10, 129.07, 127.73, 127.52, 124.15, 122.53, 121.60, 121.37, 120.81, 119.85, 119.39, 112.67, 61.85, 61.32, 21.40, 14.09. HRMS (ESI$^-$) m/z calculated for $C_{23}H_{21}N_2O_6S_2^-$ (M-H) $^-$: 485.08410, found 485.08465.

4.2.33 *2-((1-(4-methylphenylsulfonamido)-9H-carbazol-3-yl)sulfonyl)acetic acid* (**22q**)

The title compound (94.6 mg, 87.7%) was obtained as a white solid by using a method similar to that of **22i** except **22p** was used as the starting material. m.p.: 242-243 °C. ^{1}H NMR (400 MHz, DMSO-d_6): δ 11.78 (s, 1H, carbazole NH), 10.37 (s, 1H, SO_2NH), 8.54 (s, 1H, ArH), 8.22 (d, J = 7.80 Hz, 1H, ArH), 7.65-7.63 (m, 3H, ArH), 7.48 (t, 1H, ArH), 7.43 (d, J = 1.64 Hz, 1H, ArH), 7.30-7.24 (m, 3H, ArH), 4.19 (s, 2H, SO_2CH_2), 2.29 (s, 3H, PhC$\underline{H}_3$). ^{13}C NMR (100 MHz, DMSO-d_6): δ 164.58, 143.97, 140.78, 137.81, 136.56, 130.04, 129.82, 127.58, 127.52, 123.99, 122.56, 121.66, 121.29, 120.64, 119.57, 119.40, 112.60, 62.00, 21.39. HRMS (ESI$^-$) m/z calculated for $C_{21}H_{17}N_2O_6S_2^-$ (M-H) $^-$: 457.05280, found 457.05335.

4.3 Kinase Binding Assay

Compounds binding affinity with phosphorylated MEK1 (pMEK1) was performed by using homogeneous time resolved fluorescence (HTRF) assay in Proxiplate-384 F plus solid back plate (PerkinElmer) with 5 nM GST-MEK1 active (M02-10G) obtained from SignalChem, 2 nM Eu-anti-GST (Invitrogen: PV5594), 20 nM kinase tracer 236 (Invitrogen: PV5592) and test compound at a variety of concentrations. In the reaction mixture, GST-MEK1 forms a complex with the Eu-anti-GST and the tracer. Excitation of europium (the donor) by using a 340-nm excitation filter results in energy transfer to the fluorophore of the tracer. This energy transfer is detected by an increase in the fluorescence emission of the tracer at 665 nm and a decrease in the fluorescence emission of europium at 615 nm. The FRET ratio was calculated by dividing the emission signal at 665 nm by the emission signal at 615 nm. A competitor compound such as a MEK inhibitor replaces the tracer from the complex and decreases the FRET ratio accordingly. The plate was incubated in dark at room temperature for 30, 60 and 90 minutes before measuring the fluorescent emission of each well at 665 and 615 nm by using a 340-nm excitation filter, 100-µs delay time, and 200-µs integration time, on a PHERAStar plate reader (BMG Labtech, Durham,

NC). AZD6244 (Selumetinib) was used as the positive control with 100.00% ± 1.45% inhibition at 100 μM. The binding affinities of compounds at 20 μM and 2 μM were determined. Similar experiment was repeated three times. Data shown as % Inhibition normalized to AZD6244 at 100 μM. %Inhibition = 100% (DMSO-chemical)/ (DMSO-AZD6244 at 100 μM).

4.4 MEK-ERK Cascading Assay

The inhibitory effect of compounds on pMEK1 was tested by using homogeneous time resolved fluorescence (HTRF) method in which pMEK1 phosphorylates GST-labeled ERK2 directly and after the detection reagent is added, the phosphorylated ERK2 forms a complex with specific Eu-labeled anti-phospho p44/42 MAPK (Thr202/Tyr204) antibody and anti-GSTXL665. A pMEK1 inhibitor which inhibits the phosphorylation of ERK2 decreases the HTRF ratio accordingly.

Constitutively, active MEK1 (GST-MEK1, 0.4 ng/μL, Carna Biosciences) was incubated with 40 nM inactive ERK2 (Invitrogen: PV3314), 30 μM ATP, 1×enzymatic buffer, 10 mM $MgCl_2$, 1 mM DTT and test compound at a variety of concentrations. The kinase assay was carried out for 2 hours at room temperature and was terminated by the addition of 26 nM Anti-GST-XL665, 5 μL Anti-Phospho p44/42 MAPK (Thr202/Tyr204)-Cryptate (Cisbio). After 3 h of incubation, time resolved fluorescence signal was measured by a FlexStation 3 plate reader (Molecular Devices). The inhibition effects of compounds at both 20 μM and 2 μM were determined as primary result and the IC_{50}s were determined at 6 independent concentrations ranging from 5 to 160 μM. Each of the experiment was repeated three times and the calculated average value was reported as the final result. The % inhibition was calculated using equation (1) and (2). The result of positive control U0126 was consistent with previous publication[56].

$$R = \frac{\text{signal value at 688 nm}}{\text{signal value at 620 nm}} \quad (1)$$

$$\%\ \text{Inhibition} = \frac{(\text{Rpositivecontrol} - \text{Rblankcontrol}) - (\text{Rcompound} - \text{Rcompound control})}{(\text{Rpositivecontrol} - \text{Rblankcontrol})} \times 100\% \quad (2)$$

4.5 RAF-MEK Cascading Assay

The inhibition effect of tested compounds on unphosphorylated MEK1 (npMEK1) was detected in RAF-MEK cascading assay by using HTRF method with 7 nM constitutively active BRAF (Carna), 40 nM inactive GST-MEK1 (07-141-10) (Carna), 100 μM ATP, 1×enzymatic buffer, 10 mM $MgCl_2$, 1 mM DTT and the test compound at a variety of concentrations. The kinase assay was carried out for 2 hs at RT and was terminated by the addition of 26 nM Anti-GST-XL665 and 5 μL Anti-Phospho MEK1/2 (Ser217/221)-Cryptate (Cisbio). After 3 hs, time-resolved fluorescence signal was read by using FlexStation 3 plate reader. The calculation method of %inhibition in this assay is similar to that of MEK-ERK cascading assay. The inhibition effects of compounds at 20 μM or 2 μM were measured and the IC_{50}s were determined at 6 independent concentrations ranging from 2.5 to 80 μM. Each experiment was repeated three times and the calculated average value was reported as the final result.

4.6 ATP competition assay

BRaf-MEK1 cascading assay were carried out in 0.44 ng/μL active BRaf, 30 nM inactive MEK1 and various concentrations of test compound in the presence of two different concentrations of ATP (100 μM and 300 μM). The other procedures were same to that of the BRaf-MEK1 cascading assay.

4.7 Cell Viability Assay

The cell viability assays were performed with the Human Embryonic Kidney 293 cells (HEK293), human non-small cell lung cancer cell line A549, human melanoma cell line A375, and human acute promyelocytic leukemia cell line HL60, which were purchased from the Cell Bank of the Shanghai Institute of Cell Biology. The HEK293 and A375 cells were cultured in DMEM medium. The A549 cells were cultured in 1640 medium. The HL60 cells were cultured in IMDM medium. The media was supplemented with 10% fetal bovine serum (FBS), 100 units/mL penicillin, and 100 units/mL streptomycin (Invitrogen). The cells were maintained at 37℃ in a humidified environment with 5% CO_2. The cell viability was determined by using the CellTiter Glo® luminescentcell viability assay kit (Promega). Briefly, the cells were

seeded into 384-well plates at an initial density of 1000 cells/well in 50 μL of medium. Then, the cells were treated with compounds at varying concentrations. The inhibition effects of compounds at 100 μM or 50 μM were measured and the IC_{50}s were determined at 9 independent concentrations ranging from 0.39 μM to 100 μM. Staurosporine (SigmaeAldrich, catalog No. S4400) was used as a positive control. After incubation for 72 h, 20 μL of CellTiter Glo® reagent was added and luminescent signals were read on a VeriScan reader (ThermoFisher Scientific). The IC_{50} value was calculated from the curves generated by plotting the percentage of the viable cells versus test concentrations on a logarithmic scale using Origin 9.1 software.

Acknowledgments

This work was supported by the National Natural Science Foundation of China (21172012), Beijing Municipal Natural Science Foundation (7162110), and Austrian Science Fund FWF project S10711 (NFN “Drugs from nature targeting inflammation”). We also appreciate Austrian Agency for International Cooperation in Education and Research (ÖAD) to support the collaborations between these two labs.

Conflict of interest

The authors confirm that this article has no conflicts of interest.

References

[1] Robinson, M.J, and Cobb M. H. Mitogen-activated protein kinase pathways. *Curr. Opin. Cell Biol.* 9 (1997) 180-186.

[2] Cargnello M, and Roux PP., Activation and function of the MAPKs and their substrates, the MAPK-activated protein kinases.*Microbiol Mol Biol Rev*. 75 (2011): 50-83.

[3] James A. McCubrey, Linda S. Steelman, William H. Chappell, et al., Roles of the Raf/MEK/ERK pathway in cell growth, malignant transformation and drug resistance, *Biochim Biophys Acta*., 1773 (2007): 1263-1284.

[4] Roberts, P. J. and Der, C. J., Targeting the Raf-MEK-ERK mitogen-activated protein kinase cascade for the treatment of cancer. *Oncogene*, 26 (2007), 3291–3310.

[5] Davies, H., Bignell GR, Cox C, Stephens P, Edkins S, et al. Mutations of the BRAF gene in human cancer. *Nature*, 417 (2002), 949–954.

[6] Cantwell-Dorris, E. R., O'Leary, J. J. and Sheils, O. M., BRAFV600E: implications for carcinogenesis and molecular therapy. *Mol. Cancer Ther*. 10 (2011), 385–394.

[7] Ahmed A. Samatarand Poulikos I. Poulikakos, Targeting RAS-ERK signalling in cancer: promises and challenges, *Nature Reviews Drug Discovery*, 13 (2014), 928–942

[8]https://www.accessdata.fda.gov/drugsatfda_docs/nda/2013/204114Orig1s000Approv.pdf

[9]http://www.accessdata.fda.gov/drugsatfda_docs/label/2015/206192s000lbl.pdf

[10]https://www.accessdata.fda.gov/drugsatfda_docs/nda/2018/210498Orig1s000Approv.pdf

[11]http://www.fdanews.com/articles/176690-fda-awards-azs-selumetinib-orphan-drug-status

[12] Roskoski, R. Jr. ERK1/2 MAP kinases: structure, function, and regulation. *Pharmacol. Res*. 66 (2012), 105–143.

[13] Price, S. Putative allosteric MEK1 and MEK2 inhibitors. *Expert Opin. Ther. Pat.* 18 (2008), 603–627.

[14] Ohren, J.F., Chen H, Pavlovsky A, Whitehead C, and Zhang E, et al. Structures of human MAP kinase kinase 1 (MEK1) and MEK2 describe novel noncompetitive kinase inhibition. *Nat. Struct. Mol. Biol*. 11 (2004), 1192–1197.

[15] Liang, H, Liu T, Chen F, Liu Z, and Liu S. A full-length 3D structure for MAPK/ERK kinase 2 (MEK2). *Sci. China Life Sci.* 54 (2011), 336–341.

[16] Robert A. Heald, P. Jackson, and Pascal Savy, et al., Discovery of Novel Allosteric Mitogen-Activated Protein Kinase Kinase (MEK) 1,2 Inhibitors Possessing Bidentate Ser212 Interactions, *J. Med. Chem.*, 55 (2012), 4594–4604

[17] Trujillo, J.I. MEK inhibitors: a patent review 2008–2010. *Expert Opin. Ther. Pat.* 21 (2011), 1045–1069.

[18] Peng Wu, Mads H. Clausen, and Thomas E. Nielsen, Allosteric small-molecule kinase inhibitors, *Pharmacol Ther.* 156 (2015): 59-68.

[19] Duncia, J. V., Santella JB 3rd, Higley CA, Pitts WJ, and Wityak J, et al. MEK inhibitors: the chemistry and biological activity of U0126, its analogs, and cyclization products. *Bioorg. Med. Chem. Lett.*, 8 (1998), 2839–44.

[20] Redwan, I.N., Dyrager, C., Solano, C., Fernández de Trocóniz, G., and Voisin, L., et al. Towards the development ofchromone-basedMEK1/2 modulators. *Eur J Med Chem*, 85 (2014), 127–138.

[21] Ishii, N., Harada N, Joseph EW, Ohara K, and Miura T, et al. Enhanced inhibition of ERK signaling by a novel allosteric MEK inhibitor, CH5126766, that suppresses feedback reactivation of RAF activity. *Cancer Res.* 73 (2013), 4050–4060

[22] Daouti, S. Higgins B, Kolinsky K, Packman K, and Wang H, et al.Preclinical In vivo Evaluation of Efficacy, Pharmacokinetics, and Pharmacodynamics of a Novel MEK1/2 Kinase Inhibitor RO5068760 in Multiple Tumor Models. *Mol. Cancer Ther.*, 9 (2010), 134–144

[23] Daouti, S., Wang H, Li WH, Higgins B, and Kolinsky K, et al. Characterization of a Novel Mitogen-Activated Protein Kinase Kinase 1/2 Inhibitor with a Unique Mechanism of Action for Cancer Therapy, *Cancer Res*. 69 (2009), 1924-1932

[24] Lito P, Saborowski A, Yue J, Solomon M, and Joseph E, et al. Disruption of CRAF-mediated MEK activation is required for effective MEK inhibition in KRAS mutant tumors. *Cancer Cell*, 25 (2014): 697-710.

[25] http://www.rcsb.org/pdb/home/home.do

[26] Spicer JA, Rewcastle GW, Kaufman MD, Black SL, and Plummer MS, et al., 4-anilino-5-carboxamido-2-pyridone derivatives as noncompetitive inhibitors of mito gen-activatedprotein kinase kinase. *J. Med. Chem.* 50 (2007): 5090-10

[27] Ohren, J.F., Chen, H., Pavlovsky, A., Whitehead, C., and Zhang, E., et al., Structures of human MAP kinase kinase 1 (MEK1) and MEK2 describe novel noncompetitive kinase inhibition., *Nat. Struct. Mol. Biol.*, 11 (2004): 1192-1197

[28] Tecle, H., Shao, J., Li, Y., Kothe, M., and Kazmirski, S., et al., Beyond the MEK-pocket: can current MEK kinase inhibitors be utilized to synthesize novel type III NCKIs? Does the MEK-pocket exist in kinases other than MEK? *Bioorg. Med. Chem. Lett.*, 19 (2009): 226-229

[29] Isshiki, Y., Kohchi, Y., Iikura, H., Matsubara, Y., and Asoh, K., et al., Design and synthesis of novel allosteric MEK inhibitor CH4987655 as an orally available anticancer agent., *Bioorg. Med. Chem. Lett.*, 21 (2011): 1795-1801

[30] Iverson, C., Larson, G., Lai, C., Yeh, L.T., and Dadson, C., et al., RDEA119/BAY 869766: a potent, selective, allosteric inhibitor of MEK1/2 for the treatment of cancer., *Cancer Res.*, 69 (2009): 6839-6847

[31] Wallace, M.B., Adams, M.E., Kanouni, T., Mol, C.D., and Dougan, D.R., et al., Structure-based design and synthesis of pyrrole derivatives as MEK inhibitors. *Bioorg. Med. Chem. Lett.*, 20 (2010): 4156-4158

[32] Warmus, J.S., Flamme, C., Zhang, L.Y., Barrett, S., and Bridges, A., et al., 2-Alkylamino- and alkoxy-substituted 2-amino-1,3,4-oxadiazoles-O-Alkyl benzohydroxamate esters replacements retain the desired inhibition and selectivity against MEK (MAP ERK kinase)., *Bioorg. Med. Chem. Lett*. 18 (2008): 6171-6174

[33] Dong, Q., Dougan, D.R., Gong, X., Halkowycz, P., and Jin, B., et al., Discovery of TAK-733, a potent and selective MEK allosteric site inhibitor for the treatment of cancer., *Bioorg. Med. Chem. Lett.*, 21 (2011): 1315-1319

[34] Fischmann, T.O., Smith, C.K., Mayhood, T.W., Myers, J.E., and Reichert, P., et al., Crystal Structures of MEK1 Binary and Ternary Complexes with Nucleotides and Inhibitors., *Biochemistry*, 48 (2009): 2661-2674

[35] Wolber, G.; Langer, T.; LigandScout: 3-D Pharmacophores Derived from Protein-Bound Ligands and Their Use as Virtual Screening Filters. *J. Chem. Inf. Model*; 45 (2005); 160-169.

[36] https://www.ebi.ac.uk/chembldb/index.php/

[37] Lawrence, H., Ge Y, Sebti SM, and Guida W., Proteasome inhibitors having chymotrypsin-like activity. WO2010102286A2 (2010).

[38] Abulwerdi, F. A., Liao C, Mady AS, Gavin J, and Shen C, et al. 3-Substituted-N-(4-hydroxynaphthalen-1-yl) arylsulfonamides as a novel class of selective Mcl-1 inhibitors: structure-based design, synthesis, SAR, and biological evaluation. *J. Med. Chem.* 57 (2014), 4111-4133.

[39] Liu, P., Niu Y, Wang C, Sun Q, and Ping X., et al. 4-Oxo-1,4-dihydro-quinoline-3-carboxamides as BACE-1 inhibitors:Synthesis, biological evaluation and docking studies. *Eur. J. Med. Chem.* 79 (2014), 413-421.

[40] Innis, R. B. etal. Carazolol, an extremely potent β-adrenergic blocker: Binding to β-receptors in brain membranes. *Life Sci*., 24 (1979), 2255-2264.

[41] Warmus, J. S., Flamme C, Zhang LY, Barrett S, and Bridges A, et al. 2-Alkylamino-and alkoxy-substituted 2-amino-1,3, 4-oxadiazoles-O-Alkyl benzohydroxamate esters replacements retain the desired inhibition and selectivity against MEK (MAP ERK kinase). *Bioorg. Med. Chem. Lett.* 18 (2008), 6171-6174.

[42] Ge, Y., Kazi A, Marsilio F, Luo Y, and Lawrence HR, et al. Discovery and synthesis of hydronaphthoquinones as novel proteasome inhibitors. *J. Med. Chem.* 55 (2012), 1978-1998.

[43] Taylor M G, Klenke B, Suzdak P D, and Mazhari R, Cardiotonic compounds with inhibitory activity against beta-adrenergic receptors and phosphodiesterase. WO2006060122A3 (2006).

[44] Matsuo K., and Ishida, S, Synthesis of murrayaquinone-A. *Chem. Pharm. Bull.* 42 (1994), 1325–1327.

[45] Juyou Lu, Haijun Yang, Yunhe Jin, and Hua Fu, et al., Easy conjugations between molecules via copper-catalyzed reactions of ortho-aromatic diamines with ketones. *Green Chem.* 15 (2013), 3184-3187.

[46] Harden F A, Quinn R J, and Scamells P J, Synthesis and adenosine receptor affinity of a series of pyrazolo [3, 4-d] pyrimidine analogs of 1-methylisoguanosine. *J. Med. Chem.*, 34 (1991), 2892-2898.

[47] Siddalingamurthy E, Eranna M, Kittappa M, Masagalli J N, and Harishkumar H N, Mild, efficient Fischer indole synthesis using 2, 4, 6-trichloro-1, 3, 5-triazine (TCT). *Tetrahedron Lett.*, 54 (2013), 5591-5596.

[48] Kahraman, M, Borchardt A J, Davis R L, Noble S A, and Malecha J W, Carbazole inhibitors of histamine receptors for the treatment of disease. US8080566B1 (2011).

[49] Lee, K., Lee J H, Shanthaveerappa K B, Jin Xuejun and Lee J J, et al. (Aryloxyacetylamino)benzoic acid analogues: a new class of hypoxia-inducible factor-1 inhibitors. *J. Med. Chem.* 50 (2007), 1675-1684.

[50] Pipik B, Ho G J, Williams J M, and Conlon D A, A Preferred Synthesis of 1, 2, 4-Oxadiazoles. Syn.Comm. 34 (2004), 1863-1870.

[51] Sugane T, Tobe T, Hamaguchi W, Shimada I, and Maeno K, et al., Synthesis and biological evaluation of 3-biphenyl-4-yl-4-phenyl-4H-1, 2, 4-triazoles as novel glycine transporter 1 inhibitors. *J. Med. Chem.* 54 (2010), 387-391

[52] Dai Q, Xie X, Xu S, Ma D, and She X, et al., Total syntheses of tardioxopiperazine A, isoechinulin A, and variecolorin C. *Org. Lett.* 13 (2011), 2302-2305.

[53] Itoh T and Mase T, A general palladium-catalyzed coupling of aryl bromides/triflates and thiols. *Org. Lett.* 6 (2004), 4587-4590.

[54] Wagner H, Langkopf E, Eckhardt M, Streicher R and Pautsch A, et al. Arylsulphonyglycine derivatives as suppressors of the interaction of glycogen phosphorylase a with the gl subunit of glycogen-associated protein phosphatase 1 (ppl) for the treatment of metabolic disorders, particulary diabetes. WO2008113760A2, (2008).

[55] Rai G, Joshi N, Perry S, Yasgar A, and Maloney D J, et al. Discovery of potent and selective inhibitors of human reticulocyte 15-lipoxygenase-1. *J. Med. Chem.* 53 (2010), 7392-7404.

[56] S.R. Fabienne Saab, Jean-Yves Mérour, Valérie Bénéteau, and Françoise Schoentgen. Comparison of the efficiencies of two TRFRET methods to detect in vitro natural and synthesized inhibitorsof the Raf/MEK/ERK signaling pathway. *Int J High Throughput Screen*., 1 (2010), 81-98.

Highlights

- A collection of structure-based pharmacophore model of allosteric MEK1 inhibitor was constructed
- Two out of the 13 virtual hits were found active to inhibit Raf-MEK cascading
- One of the hit compound (M100) was synthesized and optimized to increase potency and to reduce cytotoxicity
- The acquired carbazole derivatives were novel in structure as allosteric MEK inhibitor
- The binding modes were analyzed by docking study